

T.C.
TED UNIVERSITY
GRADUATE SCHOOL
MECHANICAL ENGINEERING



**DESIGN AND ANALYSIS OF HARMONIC DRIVE
GEAR SYSTEM**

BERIL ARIKAN

ANKARA, 2023

DESIGN AND ANALYSIS OF HARMONIC DRIVE GEAR SYSTEM

A Thesis Submitted To
The Graduate School

of
TED University

by

Beril ARIKAN

In Partial Fulfillment of The Requirements

For

Master of Science

in

Mechanical Engineering

ANKARA, 2023

I hereby declare that all information in this document has been obtained and presented in accordance with academic rules and ethical conduct. I also declare that, as required by these rules and conduct, I have fully cited and referenced all material and results that are not original to this work.

Name, Last name : Beril Arıkan

Signature :

ABSTRACT

DESIGN AND ANALYSIS OF HARMONIC DRIVE GEAR SYSTEM

Beril Arıkan

Master of Science, Mechanical Engineering

Supervisor: Şehram Dizeci

Co-Supervisor: .Omer Music

June, 2023

This work incorporates sections on academic research, design, and numerical analysis of the Flex Spline, which is a component of the Harmonic Drive gear. The objective of this research is to minimize the Flex Spline component's both values of stress and weight while increasing the value of torque capacity by using an anisotropic composite material. Firstly, steel analysis was carried out for validation, and sample data from a reference work was used to validate the analysis results. Following that, the hybrid Flex Spline design was initiated, with composite material and adhesive resin utilized for bonding purposes. The composite materials were chosen to be carbon fiber and glass fiber, and the analytical findings were compared. Also, the adhesive bonding thickness was changed to evaluate the effects and the stress values were compared. Finally, the composite material was added while maintaining the steel rim thickness constant, and the results were compared to pure steel flex spline. The studies were carried out in two-dimensional static mode, using first and second order reduced integration. The values of the von Mises stress, plastic deformation, reaction force, contact stress, delamination, and natural frequency were examined. As a consequence of this working torque capacity increased by 20 % while stress values, contact force, and weight have decreased by 13.7 %, 11.3 %, and 38,5 % respectively thanks to the Hybrid Flex Spline.

Keywords: Harmonic Drive, Finite Element Analysis, Hybrid Flex Spline, Carbon Fiber, Adhesive Bonding.

ÖZET

HARMONİK TAHRİK DIŞLİSİNİN TASARIMI VE ANALİZİ

Beril Arıkan

M.Sc., Makine Mühendisliği

Tez Yöneticisi:

Şehram Dizeci

Ortak Tez Yöneticisi:

Omer Music

Haziran, 2023

Bu çalışma, Harmonik Tahrik dişlisinin bir bileşeni olan Flex Spline'in akademik araştırması, tasarımı ve sayısal analizi ile ilgili bölümleri içermektedir. Bu araştırmanın amacı, anizotropik bir kompozit malzeme kullanarak Flex Spline bileşeninin hem gerilim hem de ağırlık değerlerini en aza indirirken tork kapasitesi değerini artırmaktır. İlk olarak, doğrulama için çelik analizi yapıldı ve analiz sonuçlarını doğrulamak için bir referans çalışmasından alınan örnek veriler kullanıldı. Bunu takiben, birleştirme amacıyla kullanılan kompozit malzeme ve yapışkan reçine ile hibrit Flex Spline tasarımı başlatıldı. Kompozit malzemeler karbon fiber ve cam elyaf olarak seçilmiş ve analitik bulgular karşılaştırılmıştır. Ayrıca etkilerin değerlendirilmesi için yapıştırıcının kalınlığı değiştirilerek gerilme değerleri karşılaştırılmıştır. Son olarak, çelik jant kalınlığı sabit tutulurken kompozit malzeme eklendi ve sonuçlar saf çelik Flex Spline ile karşılaştırıldı. Çalışmalar, birinci ve ikinci dereceden indirgenmiş entegrasyon kullanılarak iki boyutlu statik modda gerçekleştirilmiştir. von Mises gerilimi, plastik deformasyon, reaksiyon kuvveti, temas gerilimi, delaminasyon ve doğal frekans değerleri incelenmiştir. Bu çalışma sonucunda Hibrit Esnek Yivli Dişli (Hybrid Flex Spline) sayesinde tork kapasitesi yaklaşık yüzde 20 artarken, gerilim değerleri, temas kuvveti ve ağırlık sırası ile yüzde 13,7, 11,3 ve 38,5 oranında azaldı.

Anahtar Kelimeler: Harmonic Tahrik Dişli, Sonlu Elemanlar Analizi, Hibrit Esnek Yivli Dişli, Karbon Fiber, Kompozit malzeme ile güçlendirilmiş metalik bağlama.

ACKNOWLEDGMENTS

I am deeply grateful to my advisors, Şehram Dizeci and Omer Music, for their unwavering support and guidance throughout my master's program. Their expertise and patience have been invaluable to me and have played a crucial role in the success of this thesis.

I am grateful to Türk Havacılık ve Uzay Sanayii (TUSAŞ) for providing me with the opportunity to conduct my research.

I would also like to thank . Samet Akar and Ayşe Çağıl Kandemir for serving on my thesis committee and providing valuable feedback and suggestions. Their insights and guidance were instrumental in helping me to shape my research and write this thesis.

Finally, I would like to extend my sincere gratitude to all of the participants in my study. Their willingness to share their experiences and insights has been invaluable to my research and has helped to make this thesis a success. Thank you for your time and contribution.

I am grateful to everyone who has supported me throughout this process. Without your help and guidance, this thesis would not have been possible.



To My Ati

TABLE OF CONTENTS

ABSTRACT.....	iv
ÖZET	v
ACKNOWLEDGMENTS.....	vi
TABLE OF CONTENTS.....	viii
LIST OF TABLES.....	x
LIST OF ABBREVIATIONS	xi
LIST OF FIGURES.....	xii
1. INTRODUCTION.....	1
1.1 Harmonic Drive Gears Definition	1
1.1.1 Advantages and Disadvantages of Harmonic Drive Gears.....	2
1.1.2 Working Principles of Harmonic Drive Gears.....	4
1.1.3 Application of Harmonic Drive Gears.....	9
1.2 Literature Survey.....	10
1.3 Aim and Scope	17
2. MATERIALS AND METHODOLOGY.....	20
2.1 Harmonic Drive Design	21
2.1.1 Tooth Design Geometry and Component Parameters	21
2.1.1.1 Tooth Profile	21
2.1.1.2 Flex Spline Geometry	22
2.1.1.3 Wave Generator Geometry	23
2.1.1.4 Circular Spline Geometry	24
2.1.2 Material Description	24
2.1.2.1 Steel Material Description	25
2.1.2.2 Composite Material Description	26
2.1.2.3 Adhesive Bonding.....	27
3. FINITE ELEMENT ANALYSIS.....	31
3.1 Finite Element Analysis Advantages	32
3.2 Finite Element Analysis, Design Process.....	33

3.3	Implicit and Explicit Approaches.....	37
3.4	Cohesive Zone Modelling.....	41
3.5	Validation Part	45
3.5.1	Analysis of Steel Harmonic Drive	46
3.5.2	Hybrid Design	53
4.	RESULTS AND DISCUSSIONS.....	55
4.1	Steel Flex Spline Analysis	55
4.1.1	Mesh Sensivity	55
4.1.2	Steel Flex Spline Analysis Results.....	59
4.2	Hybrid Flex Spline Analysis.....	64
4.2.1	Design Optimization.....	67
4.2.1.1	Additional Composite Reinforcement Comparison Part.....	73
4.2.1.2	Contact Force	74
4.2.1.3	Mass Reduction Comparison Part.....	76
4.2.1.4	Natural Frequency.....	77
5.	CONCLUSION.....	80
5.1	Future Work.....	81
	REFERENCES.....	82
	Ek A: Tez Fotokopisi İzin Formu	87

LIST OF TABLES

Table 2. 1 : AISI 4340 / DIN 34CrNiMo6 Steel Alloy Mechanical Properties [7]	29
Table 2. 2 : Glass Fiber Epoxy Composite Mechanical Properties	29
Table 2. 3 : Carbon Fiber Epoxy Composite Mechanical Properties	29
Table 2. 4 : Adhesive Resin Properties	30
Table 3. 1 : Plastic elongation of steel due to stress [7]	49
Table 3. 2 : The number of elements in sample data and FEM results.....	51
Table 3. 3 : The number of seeds in Flex Spline	51
Table 4. 1 : Rim Thickness Section Areas of the Optimized Flex Splines	76
Table 4. 2 : Rim Thickness Section Mass of the Optimized Flex Splines	76
Table 4. 3 : Mass Reduction on Optimized Flex Splines.....	77

LIST OF ABBREVIATIONS

HD	Harmonic Drive
CS	Circular Spline
WG	Wave Generator
FS	Flex Spline
FEM	Finite Element Method
FEA	Finite Element Analysis
CZM	Cohesive Zone Modelling
BMG	Bulk Metallic Glasses
CFD	Computation Fluid Dynamics
CAE	Computer Aided Engineering
CAD	Computer Aided Design
m_n	Tooth Module
α_l	Normal Pressure Angle
d_1	Pitch Diameter
h_f	Dedendum height
h_a	Addendum height
R_s	Design Parameter of rounded-tip
Z_i	Tooth number of i component
ζ	Rim thickness
b	Half tooth space

LIST OF FIGURES

Figure 1 : Harmonic Drive Gear [1]	2
Figure 2 : Harmonic Drive Components [1]	5
Figure 3 : Working Principle of Harmonic Drive [1]	6
Figure 4 : Normal Section of the rack cutter for Involute Flex Spline [7]	22
Figure 5 : Illustration of the neutral line with the Flex Spline and Wave Generator [7]	23
Figure 6 : Composite types based on matrices.	26
Figure 7 : Finite Element Analysis Exchanging Data Diagram [41].....	32
Figure 8 : First-Order and Second-Order Deformation Demonstration [42]	35
Figure 9 : Stress- Strain Diagram [41]	37
Figure 10 : Complexity and Efficiency for Implicit and Explicit Models [43].....	39
Figure 11 : Cohesive Zone Fracture Model [46].....	43
Figure 12 : Traction Displacement Damage Diagram [52]	44
Figure 13 : Separation- Traction Curve [53].....	45
Figure 14 : Sketch of Flex Spline Geometry	47
Figure 15 : Sketch of Wave Generator Geometry.....	47
Figure 16 : Sketch of Circular Spline Geometry	48
Figure 17 : Assembly sketch of Harmonic Drive	48
Figure 18 : Boundary conditions of Harmonic Drive components at each step	50
Figure 19: Applied Seed Distribution to Flex Spline.....	52
Figure 20: Mesh Distribution on Flex Spline	52
Figure 21 : Section Demonstration of Hybrid Flex Spline	54
Figure 22 : First Mesh Structure of Flex Spline Geometry	56
Figure 23 : Stress Analysis Results of Steel Flex Spline with First Mesh Structure	56
Figure 24 : Second Mesh Structure of Flex Spline Geometry	57
Figure 25 : Stress Analysis Results of Steel Flex Spline with Second Mesh Structure	57
Figure 26: Third Mesh Structure of Flex Spline Geometry.....	58
Figure 27 : Stress Analysis Results of Steel Flex Spline with Third Mesh Structure.....	58
Figure 28 : Stress Analysis Results of Steel Flex Spline with Second- Order Accuracy of Third Mesh Structure	58
Figure 29 : Initial Step of Harmonic Drive Assembly.....	59
Figure 30 : Harmonic Drive Assembly at the end of the Interference Step.....	60
Figure 31 : Stresses on Steel Flex Spline at the end of the Interference Step.....	60
Figure 32 : Harmonic Drive Assembly at the end of the Torque Step	61
Figure 33 : Stresses on Steel Flex Spline at the end of the Torque Step	61
Figure 34 : Strain on Steel Flex Spline	62
Figure 35 : Plastic Deformation Demonstration of Steel Flex Spline	62
Figure 36 : Variation of Stresses Occurring on the “C” point of Steel Flex Spline	63
Figure 37 : Variation of Stresses Occurring on the “F” point of Steel Flex Spline.....	63
Figure 38 : Variation of Forces Occurring on the “C” point of Steel Flex Spline	64

Figure 39 : Stresses on Hybrid Flex Spline with Carbon Fiber at the end of the Torque Step	65
Figure 40 : Strain on Hybrid Flex Spline with Carbon Fiber	65
Figure 41: Plastic Deformation Demonstration of Hybrid Flex Spline with Carbon Fiber	66
Figure 42 : Variation of Stresses Occurring on the “F” point for Hybrid Flex Spline with Carbon Fiber.....	66
Figure 43 : Stress-Strain Graph for Hybrid Flex Spline with Carbon Fiber	66
Figure 44 : Delamination Representation of Hybrid Flex Spline with Carbon Fiber	67
Figure 45 : Stresses on Hybrid Flex Spline with Glass Fiber at the end of the Torque Step ..	68
Figure 46 : Strain on Hybrid Flex Spline with Glass Fiber.....	68
Figure 47 : Stresses on Hybrid Flex Spline with 0.05 mm Adhesive Resin	69
Figure 48 : Stresses on Hybrid Flex Spline with 0.01 mm Adhesive Resin	69
Figure 49 : Strains on Hybrid Flex Spline with 0.01 mm Adhesive Resin	70
Figure 50 : Stresses on Hybrid Flex Spline with 0.4 mm Carbon Fiber	70
Figure 51 : Stresses on Hybrid Flex Spline with 0.3 mm Carbon Fiber	71
Figure 52 : Stresses on Hybrid Flex Spline with 0.2 mm Carbon Fiber	71
Figure 53: Stresses on Hybrid Flex Spline with 0.1 mm Carbon Fiber	71
Figure 54 : Maximum Stresses and Fatigue Strength Limit in Hybrid Flex Spline at Different Composite Thicknesses.....	72
Figure 55 : Maximum Stresses and Fatigue Strength Limit in Hybrid Flex Spline with 0.1 mm Composite Thickness Under Different Torques	73
Figure 56 : Maximum Stresses of Steel Flex Spline with Additional Composite Reinforcement	74
Figure 57 : Contact Force Between Contacting Surfaces in Circular Spline and Steel Flex Spline.....	75
Figure 58 : Contact Force between Contacting Surfaces in Circular Spline and Hybrid Flex Spline with 1.04 mm Steel, 0.1 mm Adhesive and 0.1 mm Carbon Fiber.....	75
Figure 59 : Contact Force between Contacting Surfaces in Circular Spline and the Flex Spline with Additional Composite Reinforcement	75
Figure 60 : First Mode of Steel Flex Spline.....	78
Figure 61 : First Mode of Carbon Fiber Flex Spline.....	78
Figure 62 : First Mode of Flex Spline when Rim Section is 0.64 mm Steel, 0.1 mm adhesive and 0.5 mm Carbon fiber	79
Figure 63 : First Mode of Flex Spline when Rim Section is 1.24 mm Steel, 0.1 mm adhesive and 0.3 mm Carbon fiber.	79

CHAPTER 1

INTRODUCTION

1.1 Harmonic Drive Gears Definition

The strain wave gear's distinctive operating theory was founded on a novel concept, it was an original idea. The group of strain wave gears encompasses the harmonic drive gear. In accordance with the idea secured by a patent granted to W. Musser, single-stage harmonic reducers were initially produced in the USA at the end of the 1950s. Musser was a creator of breakthrough ideas and concepts so he was granted awards for more than 1500 patents in science areas such as physics, chemistry, and even biology in addition to his expertise in mechanical engineering. Before he created the harmonic gear, most work on improving the speed and precision of gear mechanisms focused on making them more stable. On the other hand, the fundamental idea behind harmonic gearing was focused on making utilization of flexibility of metal and applying elastic dynamics. Because of the fact that this approach of transmitting power stood general acceptance on its head, it unexpectedly attracted attention from all across the world. Afterward, two business organizations commercialized this concept. The first one was the United Shoe Machinery Corporation (USM) which was located in the U.S.A and served as the foundation for Harmonic Drive LLC, and the second one was the Hasegawa Gear Works (HGW) which was located in Japan and which was the predecessor of Harmonic Drive System Inc.

In the world of mechanical designers, the idea of the harmonic drive has become conventional wisdom and has gained general acceptance. It has found an extensive area of usage. This newly developed mechanical transmission creates a continuous deflection wave throughout a loose gear in order to allow for gradual engagement of the teeth. Harmonic drives can produce extremely high reduction ratios in a quite small package due to this extraordinary gear-tooth meshing motion. As a side effect, this gear train's radical mechanical operation redefines how gear behavior is often understood and opens up a new field of investigation and comprehension.



Figure 1 : Harmonic Drive Gear [1]

1.1.1 Advantages and Disadvantages of Harmonic Drive Gears

Harmonic drive mechanisms stand out from other mechanical drives that exist and are used in industrial implementations due to their low overall material usage, being efficient greater than average, with torsional rigidity and low kinematic fault.

In comparison with traditional gearing, the harmonic drive gear offers several significant benefits. The extraordinarily high positioning precision and repeatability are distinguishing attributes. These are caused by the extreme transmission precision, which is more beneficial and useful than 30 arc seconds for typical series gears. The transmission precision of better than 20 arc seconds can be considered within the possibilities for a group of selected gears. The transmission precision is less dependent on the precision of many gear components or on singular tooth pitch inaccuracies, thanks to a small number of fundamental simple components and multiple tooth engagement. Classical series gears have a qualification of being repeatable between +5 arc seconds and -5 arc seconds because of extremely low hysteresis losses. The qualification of being repeatable between +3 arc seconds and -3 arc seconds can be considered within possibilities for a group of selected gears. The harmonic drive gear's ability to function without backlash enables it to acquire desired values. The gear functions smoothly because of natural radial initial loading in the area of tooth engagement. Due to the fact that power is transferred by multiple tooth engagement, harmonic drive gears offer an extreme torque capacity that is comparable to traditional

drives which are twice bigger and threefold as heavy. Harmonic drive gears have a nearly linear stiffness characteristic and high torsional stiffness. The exceptionally low internal friction in the gear installation is demonstrated by the exceedingly low hysteresis losses. Backlash in traditional gears is typically removed through external initial loading that causes an increase in hysteresis losses and loss of movement. The harmonic drive gear's efficiency is quite high in comparison to others. A harmonic gear that has a ratio of 100:1 at nominal input speed and nominal torque, being efficient over 80% is considered normal and acceptable. Being extremely efficient and having a minimum level of hysteresis losses, as mentioned previously, demonstrates that there is very little friction inside the gear structure. The teeth have fundamentally performed their function without sliding movement even at extreme speeds and have contacted nearly completely radially. Hence, loss of friction and wear are insignificant. Consequently, if the instructions prepared by the manufacturer for assembling and lubricating are followed, there will be no increase in backlash throughout the functional lifecycle of the gear. The gear has a qualification of being reversible due to its very effective speed reducer. There will be a possibility of backing-driving the gear in case of an urgent situation. The gear is the only positive drive for conveying power or the ability of movement in the group of present mechanical drives. It has been effectively utilized for many years in a great variety of equipment for numerous applications. However, the creation of gears that are slightly heavier and compact is necessary for the establishment of high accuracy and types of equipment that are relatively small. Considering the strain wave gear or harmonic drive, they can be considered as an enhancement with regard to traditional gears. Due to their high loading capacity, high-speed reduction, high torsional stiffness, high torque extension, and conveying of power in a high level, harmonic gears are used similarly to traditional gears. However, in contrast to traditional gears, all these properties can be acquired in a single stage with coaxial shafts and can be made more precisely and at lower weight. A number of several qualifications which do not cause efficiency losses such as lower level of hysteresis losses (power lost because of internal friction), no backlash, having small dimensions, being very smooth, minimum level of wear, long-lasting life cycle, high positioning precision, and being competitive in cost can be considered for harmonic gears. In summary, highly effective gearing without the need for

complicated mechanisms is allowed for by harmonic gearing. Harmonic gear can also be used for specific requirements such as transforming rotational movement into linear movement. The harmonic drive has a number of beneficial sides such as exceptional positioning precision, being repeatable, no backlash, having high torque capacity, compact design, and high single-stage reduction values. However, it has many disadvantages as well. Due to the fact that one of its constituents requires to be flexible for transmitting movement, the motion is not completely smooth here, instead, a slight ripple exists. In some implementations or frameworks of systems, the ripple causes undesirable noise and vibration. Being highly elastic, having nonlinear stiffness and damping in addition to a significantly high moment of inertia originated by the Wave Generator operation, to a certain extent of low level of power efficiency, impreciseness of kinematic, having not linear behavior can be considered among other drawbacks of harmonic gears.

Harmonic drive gears boast no backlash throughout their lifespan. They also have a few arc seconds repeatability and a positioning precision of slightly lower than one minute of arc. Harmonic drive gears are significantly smaller and lighter than traditional gears. They can achieve ratios from 30:1 to 320:1 in a single stage using just three components. Harmonic drive gears can also be made with a central hollow shaft. The hollow shaft makes it easy to run cables, supply lines, laser beams, and other objects through it.

Enhancement of a number of harmonic drive attributes can be achieved by paying attention to a convenient tooth profile. The tooth profile used in harmonic drives is essentially an involute profile. However, to enhance the interaction field and the number of teeth engagement, several researchers have adopted double-circular-arc tooth profiles.

1.1.2 Working Principles of Harmonic Drive Gears

A gear that works smoothly and with no backlash is called a harmonic drive. It is an uncommon type of gear that uses an elastic element that can be deformed to achieve a high level of reduction ratio in a single gear stage with only three basic gear components.

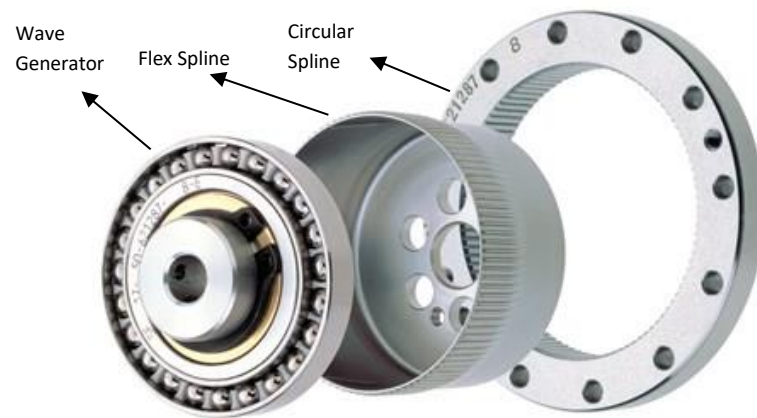


Figure 2 : Harmonic Drive Components [1]

As can be seen in Figure 2, the Harmonic Drive gear is composed of three parts:

- The Circular Spline (CS), which has a rigid cylinder-shaped ring with interior gear teeth. The Circular Spline does not move at all, as it is fastened to the main frame and held in a stationary position. It is more durable than the Flex Spline and has two more teeth overall than the Flex Spline.
- The Flex Spline (FS), which has exterior teeth made of alloy steel on the open-ended side of a slim cylinder cup. The Flex Spline is highly elastic. It is particularly stiff in torsion, but compliant in the radial direction. The closed-end side of the cup only has a flange connection to the subsequent machine parts. The Flex Spline is the fundamental part of a harmonic drive that enables the Wave Generator to produce repeating vibrations. The Flex Spline must be flexible and have an acceptable level of vibration characteristics for this purpose.
- The Wave Generator (WG), which operates as a highly efficient torque converter that incorporates a roller bearing. The Wave Generator consists of an oval plug with a thin-raced roller bearing attached. It is used as the gear's input and is also attached to the motor shaft. In addition, it functions as a torque converter with an extreme level of efficiency. The Wave Generator's interior profile is cam-shaped. It can be used to transmit torque from the Wave Generator to the Flex Spline.

The three fundamental components of the Harmonic Drive work as follows:

- The Flex Spline has two fewer teeth than the Circular Spline and a slightly smaller diameter. The teeth of the Flex Spline interact with the Circular Spline at two points on the corresponding ends of the major axis of the ellipse due to the elliptical shape of the Wave Generator.
- The interaction point of the teeth moves along the major axis of the ellipse as the Wave Generator rotates.
- For every 180° clockwise rotation of the Wave Generator, the Flex Spline rotates one tooth in the counterclockwise direction relative to the Circular Spline.
- A full rotation of the Wave Generator in the clockwise direction causes the Flex Spline to rotate counterclockwise by two teeth relative to its original position.

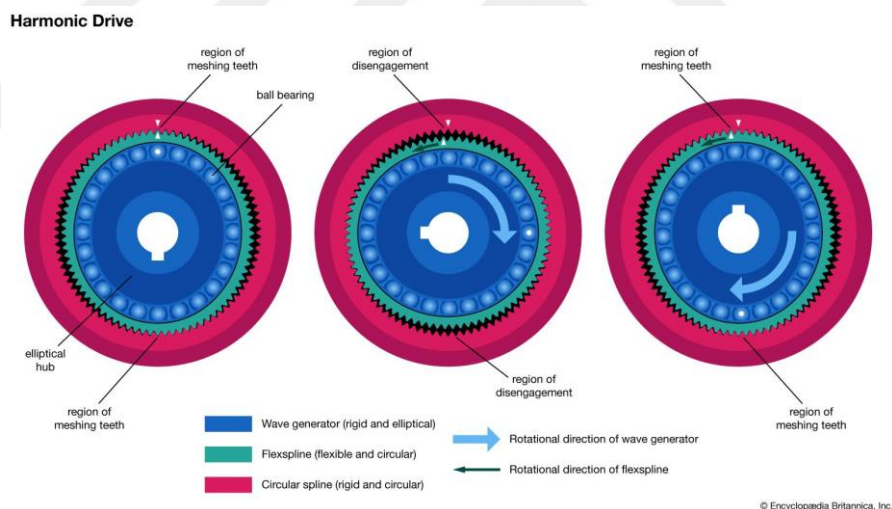


Figure 3 : Working Principle of Harmonic Drive [1]

There are more than one type of mechanical transmission, and harmonic drive is one of them. The term "harmonic" refers to the wave-like motion of the flexible component in the drive, which is caused by the rotation of the wave generator. The wave generator is a non-mechanical device that creates a wave-like motion in the flexible component. Harmonic drives are made up of flexible and non-flexible components. The flexible components are made of a material that can deform easily,

while the non-flexible components are made of a material that is stiff. The teeth of the flexible and non-flexible components mesh together to transmit power.

Harmonic drives are a relatively new type of mechanical transmission, but they have quickly become popular because of their many advantages. They are very compact, lightweight, and efficient. They also have a very high reduction ratio, which means that they can be used to transmit a lot of power in a small space.

The tooth profiles of the circular spline and the flex spline are very important for the smooth operation and transmission of power. Wave generator deforms the flex spline into an elliptical shape. The teeth of the circular spline then mesh with the teeth of the flex spline along the major axis of the ellipse.

As the wave generator rotates, the flex spline moves along the major axis of the ellipse. This causes the teeth of the flex spline to mesh with the teeth of the circular spline in a continuous manner. The flex spline is mounted on the free end side of the wave generator. This allows the flex spline to deform freely and to transmit power to the output shaft. The construction of the wave generator and the flex spline ensures that the teeth of the two components mesh together at their maximum operating level in the region of maximum deformation, and that they disengage completely in the region of minimum deformation. This results in a smooth and efficient power transmission.

The practicality of multiple contact combinations is considered, which allows for a significant reduction in the load on the tooth structures compared to other types of gear drives, and consequently, a general reduction in the size of the tooth structures. The large multiple coupling of contact in more than one area undoubtedly improves the kinematic accuracy of transmission and the smoothness of rotary motion transmission. An electrically powered mechanical device or a pneumatic drive can also serve as the Wave Generator.

The Wave Generator provides the deformation process. A Flex Spline can be a circular or thin shell. A flexible gear geometry is offered to meet a wide range of requirements, with many different designs. The Wave Generator may deform the Flex Spline in one or more areas. Additionally, the Wave Generator can be located internally or externally relative to the Flex Spline. A single-stage harmonic drive with a steel Flex Spline can provide gear ratios ranging from 60 to 600. These ratios ensure

multiple-coupled interaction. The overall number of teeth in contact is increased to approximately 40%. Kinematic errors are reduced, load capacity and efficiency are very high, and there is no empty space at the engagement area. All of these factors accurately predict the use of the harmonic drive as the final stage of the gear train. Lower vibration and noise levels are additional features.

With the exception that the Flex Spline, which symbolizes the planet gear, has a quality of flexibility, the harmonic drive is remarkably similar to an epicyclic gear train. The working principle of the Harmonic Drive is explained with the following three methods :

- 1) The most popular method uses the wave generator for input connection, a circular spline for constant connection, and a flex spline as the output connection.
- 2) The wave generator is utilized for input connection, a flex spline is utilized for constant connection, and a circular spline is utilized as the output connection.
- 3) Lastly, in the methodology that is used rarely, a flex spline serves as the input connection, a circular spline serves as the constant connection, and the wave generator serves as the output connection.

It can be supposed that the interaction between the Wave Generator and the Flex Spline is a surface engagement. As the elliptically shaped Wave Generator spins, the primary and secondary axes revolve in tandem. This results in the Flex Spline acquiring its new position by becoming untethered from the previous location of the primary axis of the Wave Generator. The tooth located at the point on the Flex Spline moves in a radial and counter-clockwise direction simultaneously.

An oval-shaped wave generator is placed into the circular open-ended side of the flex spline cup. The circular spline is then inserted into the assembled flex spline-wave generator assembly, which has an elliptical deformation. This causes the teeth to mesh (approximately 20-30% of the teeth engage) along the primary axis of interaction and separation of the teeth along the secondary axis of interaction. This is possible due to the difference in the length of the diameter and the total number of teeth between the flex spline and the circular spline. The flex spline only engages two teeth in the direction of rotation, which is in the opposite direction of the rotary movement of the wave generator. This occurs in one period of the wave generator in a harmonic drive.

Researchers use a variety of harmonic drives with different geometries and dimensions, depending on the spectrum and implementation requirements.

1.1.3 Application of Harmonic Drive Gears

It should be considered that a vehicle that performs its functionality in a space environment should have qualifications such as an extreme level of positioning accuracy, a high level of torsional rigidity, a high level of torque capacity, a lightweight and compact design, and a competitive price. Significant advancements and improvements of the harmonic drive gear can be accomplished if these aforementioned qualifications are ensured. This type of gear is a ubiquitous transmission mechanism that is utilized in many different implementation areas, such as robots used in industrial applications, printer components, medical devices, and machinery for producing semiconductor materials.

The harmonic drive gear was first used in the defense industry and air vehicles. Between 1970 and 1980, the use of harmonic drive expanded to include machine tools and industrial robotics, where it became the generally accepted standard for accurate positioning. In the 1990s, there was a sudden increase in the use of harmonic drives in areas such as measurement devices, silicon semiconductor layer processing components, and surgical robotics, as demands for greater precision and enhanced dynamic performance forced the use of high-quality gears and actuators.

The harmonic drive gear, which has its roots in aerospace, has proven itself in this industry, as it has been the best optimal option for a broad range of applications. Over approximately 50 years have passed since the first harmonic drive gears were utilized in a space environment, on the Apollo 15 mission. The Lunar Rover vehicle's single wheel drives utilized a harmonic drive as the mechanical transmission component.

The overall direction of the solar panels in spacecraft is another significant type of implementation for harmonic drive gears. In addition to single-use applications such as latch actuators, harmonic drive gears are utilized in a variety of other applications, such as making drive mechanisms for mirrors, instruments, and solar arrays.

Shortly after, harmonic drive gears were utilized in the structural mechanism of the telescope drive actuator for the photopolarimeter, which was used for imaging and

mounted on the Pioneer 10 planetary probe, which was used for a drilling mission. This actuator mechanism continued to function flawlessly when Pioneer exited the solar system in 1984.

Another classic application area is the use of electromechanical actuators for the SS/L401S satellite, which was developed as a cost-effective platform for the Globalstar global digital telephone network. The first 64 of these satellites were manufactured for use in space.

Considering the use of harmonic drive gears in renowned spacecraft such as the Hubble Space Telescope and Mars Pathfinder, this technology has proven itself and is now considered the first choice for high-power, compact positioning drives.

Surgical operations increasingly require sensitive engineering. Precision engineering helps create very precise mechanisms that can be used to perform complex tasks safely. The extraordinary performance of these systems is largely due to the outstanding qualities of harmonic drive gears.

Multiple-stage gearing drives are used to reduce the high rotations per minute of an electric motor. The use of drives with highly qualified properties such as kinematic fault tolerance, load capacity, and efficiency makes it possible to use a lower number of reducer stages in these drives. One of the best drives in terms of these characteristic criteria is the harmonic drive.

A harmonic drive is a reducer with combined gear technology. It is distinguished by its ability to achieve extremely high positioning precision and its repeatability.

1.2 Literature Survey

From the time of, the invention and gaining recognition of harmonic drive gears, numerous studies have been conducted on enhancement of performance of it by numbers of researchers. Kiyosawa et al. attempted to enhance the Wave Generator's shape and they anticipated to get better results accordingly [2]. Tuttle [3] performed a study on the characteristics of behaving of the transmission procedure to develop an analytical model for the fundamentals of operating of the harmonic drives gears. The other several researchers preferred to focus on studying the structural shape of the tooth of the Flex Spline. Nye, Ted and Robert [4] demonstrated in their study that flaws

and the geometrical structure effects in harmonic drive gear reducers gave rise to a cyclical gear error in which at a system level, resulted in high frequency torque waving. Numerous numbers of researchers focused on the stress on teeth structure of Flex Spline to determine the optimum shape of teeth for acquiring the maximum allowable fatigue life [5-6]. It was demonstrated by them that, the harmonic drive Flex Spline's Finite Element Analysis (FEA) prove that numerical analysis ensures much better anticipation of the maximum stress with respect to the experimental procedure. In addition, there are other studies about the mathematical modelling of the Wave Generator and the Flex Spline that will lead to much better performance of the harmonic drives. In their studies, Chen, Yi- Cheng, et al. [7] planned to utilize the usage of two-dimensional (2-D) finite element analysis (FEA) in order to characterize a similar qualified harmonic drive with involute Flex Spline profile. In the very initial stages, a mathematical model of the Flex Spline with an involute tooth structure profile was constructed using a straight-edge rack cutter and gearing theory. The enveloping theory and gearing theory served as the foundation for the creation of the interacting the Circular Spline with conjugated Flex Spline tooth structure profile. The Flex Spline was fitted with an elliptic shaped Wave Generator, subsequent to that, a torque was supplied to the Flex Spline in order to drive the Flex Spline meshing with the Circular Spline. Being rigid of both the Wave Generator and Circular Spline was taken into consideration in the finite element model. The performance effectiveness of the harmonic drive was measured and evaluated by utilizing the usage of the two dimensional static Finite Element Analysis that considers both the torsional angles and the torsional stiffness, and the Flex Spline's motion and fillet and engagement stresses of the Flex Spline during the meshing. In accordance with the consideration of the simulation results, the peak fillet stresses and contact stresses under a 50 N-m input torque were 577.8 MPa and 614.1 MPa respectively. Therefore, it was evidently acknowledged that they were neither greater than the yield strength nor fatigue limit of the Flex Spline material. Together with that, it was revealed that both the zones in which engagement occurred were increased and enhancement of torsional stiffness was ensured by decreasing the pressure angle of the Flex Spline, also this decrease causedless fillet stress of the Flex Spline.

A fresh approach to assess the dynamic reliability and parameter sensitivity of a device with harmonic drive which is used for the purpose of manipulation in space environment was also put out in their study by Zhao et al. [8]. This has proved that harmonic drives have played more significant roles over the coming decades, particularly in the projects which may be performed in both mechanical and aerospace projects.

Numerous numbers of studies for harmonic drive in a variety of range of topics have been continued to working on for recent years. Shortly after Maiti [9] who performed a study about split cam Wave Generator in detail in his study, Sohoo et al. [10] measured the strains of the different locations upon the Flex Spline wall surface in harmonic drive with the split cam Wave Generator by using an advanced setup. It was seen that maximum von Mises stress tensions were pretty much higher with respect to the traditional cam. Nonetheless, it was observed a significant level of reduction in the stress of engagement area of the Flex Spline with split cam. As a result, the stress generated in harmonic drive with the split cam Wave Generator nearby the tooth structure engagements was measured much lower with respect to the stress produced in the Harmonic Drive with the traditional cam.

Xu. et al. [11] studied load distribution of the Flex Spline with variety types of Wave Generator cams in their study. Studies were conducted on the effects of thin-walled component constructions of Flex Spline deformation energy dispersion. It was demonstrated by the results that, the Wave Generator cam was a significantly important parameter on the effects of deformation and carrying capacity of Flex Spline. Furthermore, it was reached the result that determination and selection of appropriate outer ring thickness might reduce the Flex Spline deformation energy dispersion.

In their study, Huang et. al. [12] preferred the utilization of usage of circumferential modification tooth structure profile instead of radial modification tooth structure profile. In this methodology, it was targeted to preserve the accuracy of the transmission and to change the service life of the harmonic drive. It was observed that with the utilization of the usage of the circumferential modification methodology, reduction could be seen in the von Mises stresses.

In their study, Kim et. al. [13] pointed out that angular transmission error was a substantially critical parameter which could be used for performance measurement. They also, explained that robot vibration could be affected by position accuracy. By using a non-contact coordinate measurement machine utilized for commercial purpose, the tooth structure profile of harmonic drive was measured and tooth structure pitch error was calculated. As a consequence, in this study, a methodology which anticipates the angular transmission error of Harmonic Drive by considering the non-contact both tooth structure profile and tooth structure engagement was proposed.

Hrcek, Slavomir et al. [14] studied a sensitivity analysis of variety of design parameters which provide the effects of lost of motion of harmonic drive. In their study, they utilized two harmonic drive gears which had equal ratio by using finite elements analysis. It was observed that, offsets used in both the Flex Spline and the Circular Spline had considerably vital effects on harmonic drive loss of motion. It was seen that, with the properly determination and appropriate selection of offsets, during the operation of harmonic drive in a preferred position, backlash reached to the ambicionado much lower value.

In another study, Li et al. [15] underlined that during its operation time the Flex Spline was exposed to the thermal load and the force load. In their study, they alleged that this situation caused undesired deformation discrepancy in both inner surface and outer surface of the Flex Spline. In order to generate a solution for this problem, the thermal mechanic connection deformation mechanism of the Flex Spline was analyzed and effects of this difference which was occurred in deformation upon Harmonic Drive transmission accuracy was studied. The proposed calculation methodology was proved itself by performing prototype tests.

In their study, Trang, ThanhTrung, et. al [16] developed a methodology based on finite elements analysis and mechanical analysis for establishment of calculation methodologies of stress for the Flex Spline. They evaluated both the durability and breakdowns of the Flex Spline. They demonstrated by matching up the simulation studies with the theoretical calculations that the peak level of stress was in the root of the tooth structure. Consequently, it could be considered that, results of this study

could be used as reference when the Flex Spline was designed and optimized for the calculation of reliability and for the evaluation of stress situation promptly.

Kim, Taesu et. al [17] proposed a new harmonic cam design application for the harmonic drive components. In this study, harmonic cam was designed by utilizing four arc combinations and it was aimed to make harmonic drive's design and manufacture easy.

Zhang, Yuxin et. al [18] developed a mathematical model for the calculations of backlash without load and they used finite element analysis in their study. They also used Abaqus software and utilized tooth structure load distribution and Hertzian contact theory for calculations.

The multiscale convolutional neural network architecture structure was used by Yang, Guo et al. [19] in order to solve the problems encountered during manufacturing and assembling of harmonic drive. Considering the results of experiments, the accuracy of the fault detection classification was observed as better with respect to other applications.

Ding, Muchan [20], developed a dynamic structural model of non-smooth harmonic drive system based on fast slow dynamical knowledge and then analyzed it. They indicated in their study, effects of parameters such as gear clearance and torsional stiffness on dynamic responses. They also provided theoretical models within the scope of his study for enhancement the transmission precision and consistency of Harmonic Drive.

Kuo, Jong-Yih, et al. [21] designed a model which can be used to test that the Harmonic Drive had fault or not. Within the scope of this study it was aimed to use the recorded voice utilizing a microphone for testing the gear failure of Harmonic Drive. Then, examples of recorded voices separating from noise were tested by experiments.

In their study, Tang, Ting et al., [22] proposed a novel model for capturing transmission compatibility, hysteresis and degradation by considering the effects of engagement of Harmonic Drive and the multi tooth structure meshing. There were

crucial parameters considered in this proposed novel model such as engagement, Wave Generator stiffness and friction coefficient. If it is aimed to design a Flex Spline, it should have a qualification of flexibility on radial movement direction and have qualification of stiffness on torsional movement direction. It has possibility that the harmonic drive gear can be considerably increased its qualifications by carefully choosing its geometrical specifications, while also utilizing suitable materials, isotropic materials like steel, or technical procedures. Because of this reason, academical investigation studies about Flex Spline's material selection have been proposed and it could be considered that material selection plays enormously vital role in Harmonic Drive.

In their study, Hofmann, Douglas C., et al. [23] proposed the utilization of bulk metallic glasses (BMGs) just as strain wave gear material. According to recent study, bulk metallic glasses can be manufactured at incredibly low costs when compared with machining and are utilized as a replacement to steel in harmonic drive gear. By using this methodology, it was anticipated that an enormous decrease in cost could occur. The main topics of the essay were how to save costs, improve performance in the envisioned environment, minimize the mass, incorporate new materials, and create drives which are pretty smaller with respect to previous ones. An investigation study of feasibility was performed to determine bulk metallic glasses could be efficiently and effectively constructed from a numerous type of distinct alloys into the Flex Spline for evaluating the potential and about 60 BMG Flex Splines were manufactured. In this study it was demonstrated that, although being inherently fragile, BMGs were capable of transmitting torque in case employed as the Flex Splines, because of their strength and elastic strain limit. This was accomplished by creating a BMG Flex Spline prototype and using it on a NASA JPL robot, where it successfully completed a limited number of cycles.

In their innovative method, Oh, et al. [24] suggested employing glue between composite and steel components to create the harmonic drive's Flex Spline part. The adhesive-bonded Flex Spline was founded to have adequate torque transmission capabilities, and both the composite and the bonded steel Flex Spline outperformed the one-piece steel Flex Spline in terms of dynamic performance. It was proposed by

them that the Flex Spline's composite component would boost the natural frequency distribution and damping capability. Adhesive bonding and hybrid Flex Splines were the methods employed. Epoxy resin IPCO 9923 was used for bonding and thicknesses of 0.1, 0.5 and 1.0 mm were chosen. Considering the results of experiments, hybrid Flex Splines have adequate transmission qualification and rotational rigidity, inherent frequency was improved with respect to the traditional ones.

In their study, Jeong, et al. [25] demonstrated that the constructed composite Flex Spline outperformed the one-part steel in terms of having radial flexibility and having extreme level of damping capacity at the essential inherent frequency. In addition to that, the composite Flex Spline's mass value was reduced with respect to the steel Flex Spline. Jeon, Han Su, and Se Hoon Oh [26] reached nearly identical results figures in case they explored the stress analysis and vibration properties of the Wave Generator utilizing ANSYS which is a finite element analysis tool used for commercial purposes for numerous types of situations. The analysis was performed through two types of models such as first one was a steel Flex Spline and the second one was a steel composite hybrid Flex Spline model. The second one was tied to the inner part of the Flex Spline. It could be concluded from the results that, the carbon fiber epoxy hybrid model's von Mises stress was measured as 5,73% lower with respect to the steel model and the former's inherent frequency was measured as higher 7.7 times when compared to the latest. The hybrid steel-composite model had a displacement that was 23 times less than the steel variant.

Folega P. and G. Siwec [27] in their study utilized an approach methodology considering the finite element and they used MSC Patran/Nastran software tool for performing the impact on the Flex Spline steel and steel-composite materials on Flex Spline strength for both two- and three-dimensional models. Calculations mentioned above were conducted on in two parts. The first part was considered as related with Flex Spline-Wave Generator engagement's models with two dimensions. The second part was considered as related with Flex Spline models with three dimensions. Steel was strengthened employing a composite substance, and epoxy resin was the material of choice for adhesive bonding. The thickness of the epoxy resin was not specified. Teeth structure was not considered during the modelling of the Flex Spline. The von

Mises stresses of a hybrid Flex Spline, that was made up of a pair of composites structure with a resin made of epoxy strengthened by carbon-fiber or glass-fiber, were reduced while vibration frequency grew higher. In cases where the stacking fiber angle was 75 degrees, the biggest decrease in stress values observed. Moreover, Folega P. [28] further emphasized the importance of the Flex Spline's vibration attributes and flexibility characteristics. In this paper, comparison evaluation was performed in terms of the steel-composite and steel Flex Spline values for inherent frequency and torsional angle. With respect to the conventional Flex Splines, weight of the Flex Spline was reduced, inherent frequency grew higher and torsional angle was reduced. The employing of composite materials was emphasized as an effective way of strengthening torsional stiffness. In return for worries related to the manufacturing of complete composite Flex Spline. They advocated that the utilization of hybrid Flex Spline strengthened with composite material.

On harmonic drive gear, several studies have been conducted, including tooth profile synthesis, load sharing analysis, stress, strain, and torque analysis design. In contrast to other research, in this study, weight reduction study was carried out in Flex Spline and anisotropic material was added by reducing the steel material thickness and the analysis results were examined.

1.3 Aim and Scope

In addition to the vehicles that are used in space environments, ongoing developments in harmonic drive technology have broadened its potential utilizations to other areas demanding extremely precise rotational positioning. The harmonic drive gear, which originated in aerospace, has recently proved itself as an effective and efficient solution in a numerous variety of distinctive scenarios. It can be concluded that the technology of designing and producing these types of gear systems has not yet been developed in Turkey, and that this is one of the major weaknesses.

As previously stated, FEM analysis makes it possible to reduce the weight by optimizing all gear components. Decreasing the thickness makes it possible to reduce the weight of the Circular Spline. Additionally, if desired, the width of the teeth structure of the Circular Spline can be reduced. Reducing the thickness value of the flange at the closed end side of the cup can lead to a decrease in the overall mass value of the Flex Spline. The overall mass value of the Wave Generator can also be decreased by eliminating the Oldham coupling that is frequently incorporated within the plug and by optimizing the cross-sectional profile design.

Considering the components of the harmonic drive gear, it could be concluded that the Flex Spline is one of the fundamental constituents among all components for the transmission of the movement. It must have a qualification of flexibility in the radial direction. In addition, it must have a qualification of high stiffness in the torsional direction for precisely conveying rotary movement.

For the fulfillment of this multiple purposes, the steel Flex Splines are frequently produced in a cup shape with a small dimension and necessitates extensive drilling and hobbing processes employing particular jigs.

Although the harmonic drive gear offers numerous number benefits, it has one disadvantage: the movement is not incredibly smooth; however, it has a small waving inasmuch as the Flex Spline has to have a qualification of being flexible in order to transfer the movement. In robot systems and other systems that make use of harmonic drives as tool used for speed decreasing purpose, the ripple can cause vibration and noise. Due to the fact that contradictory dual role could not be fulfilled effectively and efficiently through traditional isotropic substances and materials, this could be accomplished through utilization of anisotropic composite materials and substances.

Within the scope of this thesis, the application areas for harmonic drive gears were focused on and were evaluated in detail. A literature review considering the accessible studies were given and the details of the harmonic drive were demonstrated. In the second part, information regarding the steel and the composite materials utilized in different stages of the manufacturing were presented. The main purpose of this thesis is to minimize the overall mass value of the Flex Spline and enhance its torque

capability. In the finite element analysis section of this study, the harmonic drive sample proposed in a paper published by Chen, Yi-Cheng, et al. [7] was constructed through a numerical model using a finite element solver. The stresses on the Flex Spline were simulated during the validation stage to ensure the verification stage was valid enough. Following completion of the validation step, the carbon fiber and glass fiber epoxy composite materials were used to manufacture the Flex Spline's cup, and the steel material was used to create the component's teeth. Both components mentioned previously then were attached by using adhesive bonding. For optimizing the design and increasing the performance, the finite element method was utilized. Design improvement studies were carried out to minimize stresses and increase the torque transmission ratio at the design improvement section by studying the analytical findings of the hybrid Flex Spline model. Consequently, the section under "Results and Discussion" examines the analytical and numerical results that were obtained within the scope of this study.

CHAPTER 2

MATERIALS AND METHODOLOGY

This thesis study was planned to have three main sub-parts such as research, design, and eventually analysis. In the first part, relevant articles about the harmonic drives were reviewed and the manufacturers of harmonic drive gears were investigated. During the research and review period of the relevant articles regarding harmonic drive, the reliability of those articles was also taken into consideration as well. Subsequent to all the information regarding the gear and its components, the studies were planned to clarify how gear design conducted, and which parameters were critical ones.

During the design phase, a sample of harmonic gear design was chosen from among all the data gathered during the literature review phase. Within the design, it was concluded that the parameters such as the number of teeth, the gear module, the pitch diameter, rim thickness, pressure angle, and the structure of the tooth have substantially crucial roles. In the reference work [7], there were remarkable parameters for the design of each three components. Section 2.1 demonstrates a detailed explanation of the gear design process. Furthermore, the materials and substances that may be used in the harmonic drive gear during the design phase were also explained as well. As it was mentioned in Section 1.3, it was aimed to conduct some design improvements regarding the harmonic drive gear by changing the materials of the Flex Spline and consequently, increase the performance of the harmonic drive gear.

Eventually, the third phase of this thesis includes the analysis section for the verification of data and new advancements are proposed. Abaqus/CAE 2021 software tool was used for the finite element analyses where the static and the dynamic analyses, the cohesive zone modeling, mesh quality, and the sensitivity were researched. The analysis section includes the validation of the reference data and the improvements performed subsequently. Detailed information regarding this phase can be seen in section 3 Finite Element Analysis Method.

2.1 Harmonic Drive Design

As indicated before, harmonic drive gear is designed with three components as a compact construction. The Wave Generator, one of the Harmonic Drive components, takes a role as torque converter. This ball bearing with elliptical cam typically receives the power from a servo motor. The Wave Generator is fitted into the Flex Spline and the Flex Spline takes the elliptical shape of the Wave Generator. Rotation of the Wave Generator drives the Flex Spline, and the Flex Spline mates with the Circular Spline teeth. The Circular Spline has the same major axis as the Wave Generator and torque transmission occurs at mating surface.

2.1.1 Tooth Design Geometry and Component Parameters

2.1.1.1 Tooth Profile

The tooth profile is one of the important parameters for gear design. Tooth profile affects torque transmission, stress, gear durability, performance, and so on. There are some methodologies for shaping gear teeth. Therefore, there are lots of tooth profiles for gears. Some of them are involute tooth profile, conjugated tooth profile, cycloidal tooth profile, and arc of circle tooth profile. The gears are thought to have conjugate action if the tooth profile of a set of gears is built in such a way that a constant angular velocity ratio is generated and maintained during operation. As a result, the teeth of such gears that conduct conjugate action are understood to have a conjugate profile. A cycloid is a curve formed by rolling a point on a circle on a straight line without sliding. A gear tooth with a cycloidal profile is one that follows a cycloid curve on its matching gear. By connecting an imaginary tight thread to the supplied curve and following its open end as it is unraveled from the given curve, an involute curve is generated. The gears that track an involute curve are referred to as involute profiles. The tooth is a cylindrical arc with a circular contour that meshes with the other gear. A convex arc may sometimes fit within a concave arc for improved transmission. Moreover, pressure angle is an essential tooth profile design

characteristic because it determines the angle at which forces are transferred between meshing gears [29].

2.1.1.2 Flex Spline Geometry

The Flex Spline is one of the critical component of the Harmonic Drive. Within the scope of the thesis, straight-edged rack cutter whose tooth profile is shown as Figure 3 was used to generate the involute Flex Spline tooth profile. Straight edged rack cutter was considered to generate the involute Flex Spline teeth profile [7]. With this method, straight edged rack cutter has cutting profile, and the Flex Spline moves onto straight edged rack cutter. Rack cutter cuts out material from the Flex Spline surface and the Flex Spline tooth profile could be generated to match with rack cutter. In the reference harmonic drive gear design article [7], the pressure angle was set at 20 degrees. Pressure angle effect tests were conducted at 16, 18.75, 21.5, 24.25, and 27 degrees in addition to 20 degrees in reference article.

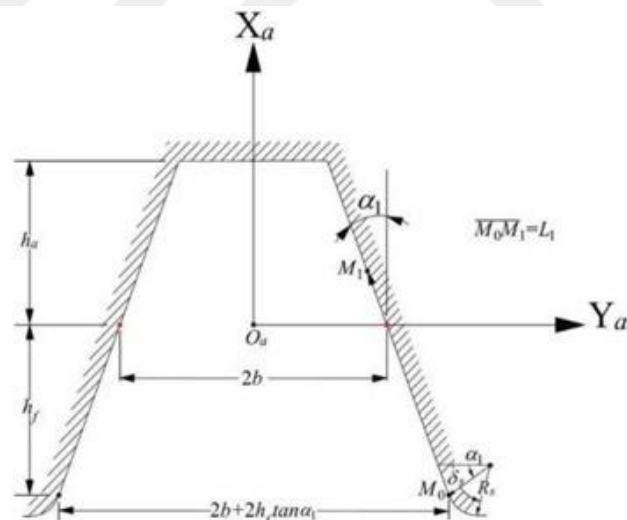


Figure 4 : Normal Section of the rack cutter for Involute Flex Spline [7]

Thanks to a number of teeth difference between the Flex Spline and the Circular Spline, which is 2, a high torque transmission ratio can be produced. In this study, the Flex Spline has 200 teeth and the Circular Spline has 202 teeth [7]. Therefore, the torque transmission ratio of the Harmonic Drive is 100.

$$\text{Tooth Module } m_n = 0.5 \quad (2.1)$$

$$\text{Normal Pressure Angle } \alpha_l = 20^\circ \quad (2.2)$$

$$\text{Pitch Diameter } d_1 = 100 \text{ mm} \quad (2.3)$$

$$\text{Dedendum height } h_f = 0.48 \text{ mm} \quad (2.4)$$

$$\text{Addendum height } h_a = 0.5 \text{ mm} \quad (2.5)$$

$$\text{Design Parameter of rounded-tip of Rack Cutter } R_s = 0.14 \text{ mm} \quad (2.6)$$

$$\text{Flex Spline tooth number } Z_{fs} = 200 \quad (2.7)$$

$$\text{Circular Spline } Z_{cs} = 202 \quad (2.8)$$

$$\text{Rim thickness } \zeta = 1.24 \text{ mm} \quad (2.9)$$

$$\text{Half tooth space } b = \frac{\pi m_n}{4} \quad (2.10)$$

Parameters [2.1-2.9] and equation [2.10] were taken from the article [7]. With using of these parameters, the Flex Spline design was completed.

2.1.1.3 Wave Generator Geometry

The Wave generator is basically rotating elliptical component of the harmonic drive. In this case, the Wave Generator forces to deform neutral line of the Flex Spline. For a full shrinkfit, the Wave Generator perimeter is assumed as same with neutral line of the Circular Spline. Following equations are used to design the Wave Generator.

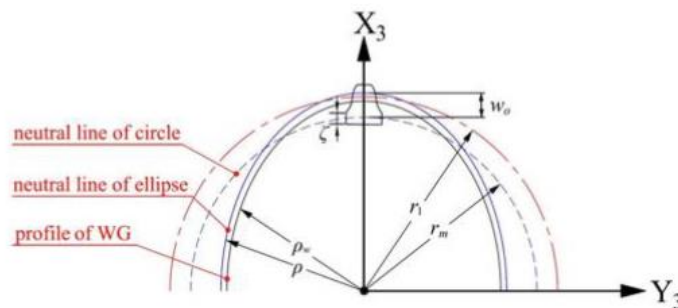


Figure 5 : Illustration of the neutral line with the Flex Spline and Wave Generator [7]

Distance between deformed ellipse and undeformed neutral line of circle

$$w_0 = 0.625 \text{ mm} \quad (2.11)$$

Pitch radius of undeformed Flex Spline $r_1 = \frac{d_1}{2} = 50 \text{ mm}$ (2.12)

The distance between center and neutral line of Flex Spline

$$r_m = r_1 - h_f - \frac{\zeta}{2} = 48.82 \text{ mm} \quad (2.13)$$

The radial vector of the neutral line of ellipse of the deformed Flex Spline

$$\rho = r_m + w(\theta) = r_m + w_0 \cos(2\theta) \quad (2.14)$$

$$\theta = 0, \quad \rho_{max} = r_m + w_0 \quad (2.15)$$

$$\theta = \frac{\pi}{2}, \quad \rho_{min} = r_m - w_0 \quad (2.16)$$

Maximum radius of inner surface of Deformed Flex Spline

$$\rho_{w_{max}} = \rho_{max} - \frac{\zeta}{2} \quad (2.17)$$

Minimum radius of inner surface of Deformed Flex Spline

$$\rho_{w_{min}} = \rho_{min} - \frac{\zeta}{2} \quad (2.18)$$

2.1.1.4 Circular Spline Geometry

The Circular Spline tooth profile is designed to conjugate with the Flex Spline tooth profile. Main design parameters of Circular Spline are the number of tooth and it is selected as 202 and therefore, pitch diameter is calculated as 101 mm.

2.1.2 Material Description

The materials of the harmonic drive gear are critical. Composite will be utilized in the Flex Spline material in addition to the standard harmonic drive steel materials.

The Wave Generator and circular spline are made entirely of steel. The Flex Spline is made of composite and steel materials. An adhesive bonding is used for joining certain materials together.

2.1.2.1 Steel Material Description

Steel is an alloy distinctively consisting of iron and carbon. The percentage of the carbon present in the steel varies between 0.02% and 2.14% [30]. The percentage of perlite in the chemical composition increases until the percentage of carbon increases to % 0.80 – 0.85 [31], the tensile strength and the yield strength of the steel increases. Steel is a ductile material which can have certain amount of elastic deformation before fracture. However, increasing the amount of carbon reduces the ductility of the part. Therefore, part becomes more brittle.

According to the usage areas of steel, different steel alloys have been developed. Steels can be divided into two groups which are called the low steel alloys and the high steel alloys, and these groups are determined according to the amount of alloy. Manganese alloy improves ductility, hardness, wearing resistance. Manganese alloy is suitable for the machine tools. Sulphur alloy makes parts more brittle but machineable. Manganese can balance ductility. Nickel develops strength, toughness. Crom provides more strength hardness and corrosion resistance. Crom can be good pair with Molibden and Nickel. Molibden also improves strength and hardness. Vanadium and Silicium increases the strength without reducing ductility. Beside, Silicium increases fluidity.

Compared with other materials, the mechanical properties of steel are high. The tensile strength of a material is the strength at which the material can undergo deformation without fracture. The tensile strength of steel is quite high compared to other materials. The density of steel varies in the range between 7,750 and 8,050 kg/m³ [32].

2.1.2.2 Composite Material Description

New materials obtained by physically mixing at least two different materials with each other are called the composite materials. Unlike alloys, chemical dissolution does not occur in the materials that make up the composite. Composites basically consist of two components. These are the matrix and the reinforcement element. Thanks to the reinforcement element, the insufficient mechanical properties of the matrix material such as strength, toughness, weight, conductivity are improved.

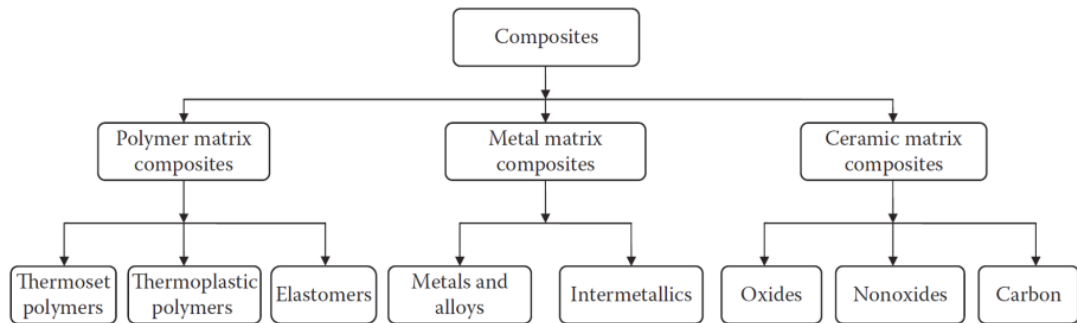


Figure 6 : Composite types based on matrices.

Composites are divided into three groups according to matrix types. The first one is polymer, the second one is metal and the last one is ceramic matrix composites. Ceramic matrix composites are very useful because they are resistant to high temperatures and are lightweight. Ceramic-based composite materials are commonly used for parts that must operate at high temperatures. Because they are hard and brittle, they have very low ductility and toughness and are not resistant to thermal shock. For this reason, they are mostly enriched with fibers. On the contrary, they have a very high modulus of elasticity and very high operating temperature. Ceramic composites have very good resistance to high temperatures but have a rigid and brittle structure. In addition, they exhibit very good electrical insulating properties.

Second, polymer matrix composites are primarily petroleum-derived products and are currently the most widely used materials. Polymer composites are materials that are resistant to corrosion, suitable for long-term use, easily processed, molded,

and have a high bearing capacity per unit mass [33]. Thermosetting matrix composites and thermoplastic matrix composites are the two types of polymer matrix composites. Thermoset matrices are more used in the production of fiber-reinforced composites and are in liquid form, with the addition of a hardener, they first become gel and then harden. Thermoset resins are isotropic.

Lastly, Metal-matrix composites are designed mixtures of two or more elements (one of which is a metal), with tailored qualities acquired through systematic combinations of distinct elements.[34]

The most common type of composite materials are fiber-reinforced composites. In fiber-reinforced composite materials, the constituent materials differ from each other in molecular size and can be mechanically separated from each other. The matrix (resin) may be thermoset or thermoplastic. Reinforcing fibers are made from long fibers, woven fabrics, short fibers, etc. They come in a variety of shapes. Each format results in separate functions. The properties of a composite material depend on how the fibers lie within the composite, in other words, which layout is selected for fibers within the composite. The winding direction of the fiber changes, the mechanical strength, and the amount of deformation.

Carbon fiber (graphite fiber) is a long thin fiber of material approximately in diameter, made up primarily of carbon atoms. Carbon fiber is made up of a combination of thousands of fibers. The carbon fiber of the same strength is five times stronger and twice as hard as steel. Although it is stronger and harder than steel, it is lighter than steel. Its light weight makes it an ideal material for many parts. Carbon fiber has high stiffness, high tensile strength, high strength-to-weight ratio, and high corrosion resistance. Carbon fiber is a perfect selection for the aerospace, defense, marine, and automotive industries.

2.1.2.3 Adhesive Bonding

Adhesive bonding is the technique of joining two or more components by solidifying or hardening a non-metallic adhesive material put between the faying

surfaces of the parts.[35] Epoxy resin is the most commonly used adhesive bonding used for bonding various materials. It acts as a strong adhesive due to its ability to increase the attractive force between bonds, which belongs to the group of thermoset materials in engineering applications. They exhibit excellent resistance to moisture, heat, chemicals, and abrasion and have a long service life. Fiber-reinforced epoxies can use all types of fibers and use epoxy as the matrix material. The outer gear of harmonic drive, circular spline, is generally constructed of steel. Materials like C45, C55, and 28Cr4 are used frequently [27]. Hu, Guyue, et al. Studied the dry friction and wear characteristic of ductile iron for two types of harmonic reducers at room temperature compared to 40Cr alloy steel for the circular spline and as a result of the investigation, ductile iron has better wear resistance [36]. The Wave Generator is made up of a thin racing ball bearing that is mounted onto an elliptical shaft [37]. Therefore, the material of the Wave Generator is determined based on the bearing materials which have high rolling fatigue strength. The Flex Spline material is the most important issue considering all components of the Harmonic Drive. 42CrMo4, 35CrMo4, 34CrNiMo6, 40NiCrMo6 materials are especially used [27]. A significant amount of harmonic drive material selection studies are centered on Flex Spline material.

In this study, the circular spline and the Wave Generator are defined as 2d rigid bodies. Thus, there is no need to select material for these two components of the harmonic drive. The Flex Spline material is the focal point of this work. First of all, a reference work was selected to validate the analysis. The Flex Spline material used in this article is steel. its modulus of elasticity is 200 MPa and Poisson's ratio is 0.29. In addition, it is stated in the article that the fatigue limit of the steel material is 640 MPa and the yielding strength is 860 MPa [7]. However, the type of steel is not specified. In light of this information, it is thought that AISI 4340 (34CrNiMo6) steel was selected by investigating the steel material properties. Table 2.1 indicates the AISI 4340 mechanical properties which was taken by T. Özel et al. [38] article. AISI 4340 steel ultimate tensile strength is used for defining plastic deformation material parts in Abaqus. It was taken at 1282 MPa.

Table 2. 1 : AISI 4340 / DIN 34CrNiMo6 Steel Alloy Mechanical Properties [7]

AISI 4340 / DIN 34CrNiMo6 Steel Alloy	
Modulus of Elasticity	200 GPa
Poisson's Ratio	0.29
Yield Strength	860 MPa
Density	7.8 g/cm ³

Secondly, As it is known, the Harmonic Drive is a structure used in the robotics and space industry. The most sought-after features in these sectors are weight, strength, low cost, and resistance to vibration. For this purpose, a preferable Harmonic Drive design was investigated within the scope of the thesis. When parameters such as weight, strength, and longevity are taken into consideration, the first material that comes to mind is composite. For a better-performing, Harmonic Drive, the interior of the Flex Spline was modeled with carbon fiber epoxy composite and glass fiber epoxy composite. Considering the requirements of the Harmonic Drive design, epoxy adhesive was selected.

Table 2.2 demonstrates the glass fiber mechanical properties which was taken by Sun, X. S., et al. [39] article.

Table 2. 2 : Glass Fiber Epoxy Composite Mechanical Properties

E1[MPa]	E2[MPa]	E3[MPa]	Nu12	Nu13	Nu23	G12[MPa]	G13[MPa]	G23[MPa]
48700	16800	16800	0.28	0.28	0.4	5830	5830	6000

Table 2.3 shows the carbon fiber mechanical properties which was taken by Yahya, N. A., and Safa Hashim [40] article.

Table 2. 3 : Carbon Fiber Epoxy Composite Mechanical Properties

E1[MPa]	E2[MPa]	E3[MPa]	Nu12	Nu13	Nu23	G12[MPa]	G13[MPa]	G23[MPa]
139400	7660	7660	0.26	0.26	0.306	3680	3680	2940

Table 2.4 shows the adhesive resin mechanical properties which was taken by Yahya, N. A., and Safa Hashim [40] article.

Table 2. 4 : Adhesive Resin Properties

Adhesive Bonding	Young Modulus MPa	Shear Modulus MPa	Shear Modulus MPa
Epoxy resin Araldite LY3505/XB3405	3500	1296	1296
Epoxy adhesive Araldite 2015	1800	662	662

CHAPTER 3

FINITE ELEMENT ANALYSIS

Various approaches are used by engineers all around the world to be able to analyze different types of problems, such as structural and thermal, encountered during the design process. Design analysis is the practice of analyzing the specific qualities of certain components or assemblies. For design analysis, genuine components or models that simulate specific aspects of real objects might be employed. Through the utilization of models instead of components or items which are used in the real world, the analysis may be performed during the beginning of the design processes, prior to manufacturing of the final product, even before the prototypes are built. These models can be divided into sub-groups such as physical (scaled-down models, mockups, photo-elastic models, etc.) or mathematical (a mathematical apparatus describes the behavior of a part or assembly).

Design analysis conducted using the mathematical models can be further divided into sub-groups based on the consideration of methodologies that are utilized to obtain a result. As a consequence of calculations by using simple mathematical models, analytical solutions can be acquired. It can be concluded that, in order to obtain results from the utilization of more complicated methods, numerical approaches are to be embraced. The finite element analysis (FEA) is considered one of the numerical approaches which are utilized for solving the more complicated models [41].

FEA is employed as one, among other several computer-aided engineering (CAE) software tools that benefits mechanical design activities. Analysis of fluid flow which is most usually known as computation fluid dynamics (CFD) and the mechanism analysis are accepted as two further CAE technologies. All these significant three key CAE technologies aforementioned above are connected with computer-aided design (CAD), which serves as a hub for all CAE applications. CAD and add-ins, as well as directly between various add-ins, may communicate geometry and material characteristics. The numerical techniques that are used in FEA, CFD, and

mechanism analysis were developed separately from each other. Even though CAE tools are stand-alone applications rather than CAD add-ins, both of them can nevertheless have an interface with CAD. It can be expressed that the primary matter which causes the distinction between FEA and motion analysis is the domain of application. Structures that are sensitive to loads are examined using finite element analysis (FEA), and mechanisms' motion is examined using motion analysis [41]. The below figure demonstrates the data diagram's relation with FEA.

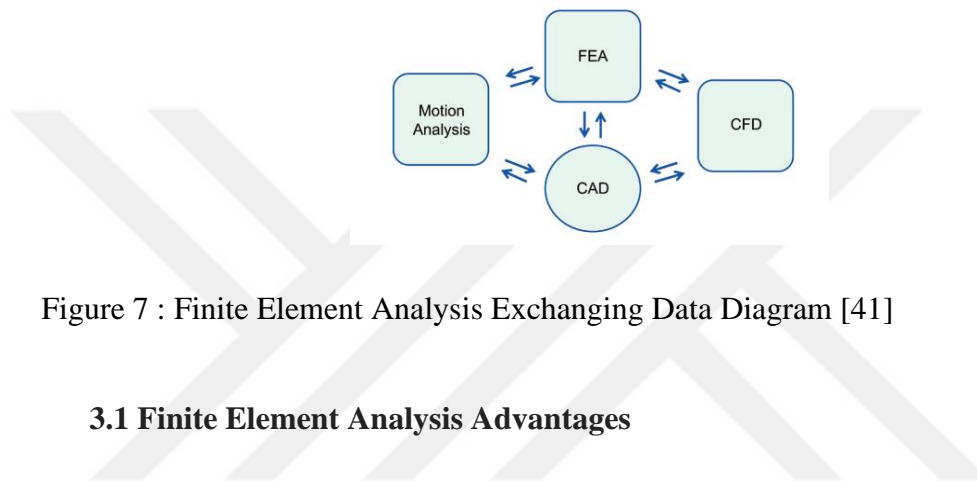


Figure 7 : Finite Element Analysis Exchanging Data Diagram [41]

3.1 Finite Element Analysis Advantages

The finite element analysis (FEA) methodology can be defined as applying the process of simulating a part or assembly's behavior under certain kinds of loading conditions. FEA utilizes mathematical models to comprehend and evaluate real-world loading effects on a part or assembly. In design activities, engineers can identify different types of possible issues, such as stress concentration points and weak spots. FEM is utilized effectively for modeling the structures such as complex geometrical and asymmetrical shapes. Through the use of FEM, it could be ensured that a complex geometrical-shaped structure with unidentified structural behavior can be broken down into a finite number of simple geometrical-shaped pieces with identified structural behavior. A matrix equation is developed by ensuring equality of the displacements at the element borders with the adjacent elements. A post-processor is employed in order to make the results of the numerical solutions more visual. Once the forces are applied to the model, the results of the computed stresses, strains, and displacement are demonstrated for the review process.

Engineers prefer to utilize the FEA to reduce the requirement for actual prototypes where the optimization process turns out to be more simple and feasible.

The advantages of FEA can be considered as followings:

- The problem can occasionally be impossible to be solved when the geometry is complex. FEA can produce results more quickly and with high precision in these conditions.
- Solutions can be produced by making modifications to the parameters of a developed FEM model, and these solutions can then be evaluated and compared to consider the parameter effects.
- FEA enables designs to be optimized in accordance with the requirements and produces effective design solutions.
- FEA can provide enhancement in the component strength and life, reduce component weight, reduce cost, improve quality, and validate design solutions for different parts and assemblies.

With different solutions, FEA methodology can be commonly used to conduct a wide variety of analyses. Types of analysis such as both static and dynamic structural analysis, thermal analysis, modal analysis, fluid analysis, and acoustic can be considered as examples of different types of analysis mentioned previously. Because of the fact that having a qualification of being able to conduct many different types of analyses.

3.2 Finite Element Analysis, Design Process

To be able to begin an FEA project, a CAD model which serves as the primary material for developing the structure of a mathematical model is significantly required. It is important to explicitly define what a mathematical model is and to demonstrate how this mathematical model fits into the design analysis process. In addition to that, it is also critical to explain how the mathematical model differs from the CAD models and finite element (FE) models to emphasize and underline the significance of it the analysis process. A volume is defined through the utilization of a CAD model. In addition to having certain requirements established on each exterior face that delineates domain borders, the volume has material attributes allocated to it. Boundary

conditions are described as the conditions that are specified on a model's outside faces. Both displacements and loads can be beneficial to determine the boundary conditions. The terms "essential boundary conditions" and "natural boundary conditions" are employed to describe displacement and load boundary conditions, respectively [42].

The fundamental of the FEM methodology is established by the variational formulation of a boundary value issue. The unknown functions in the FEM are modeled by polynomial-derived functions. On account of the fact that these functions have a qualification of numerical efficiency, they can be considered practical and beneficial. It is necessary to discretize (or meshed) the complete solution domain into easily formed subdomains known as elements. Polynomial functions would have to be quite complicated to describe the whole model "in one piece" without breaking it into components. At this point, the necessity of meshing is clear and can be thought of as inevitable. Meshing divides the solution domain into easily formed components or subdomains, allowing for the approximation of the displacement or temperature field in each element using relatively simple polynomials. Discretization provides mesh geometry, even though it is not just applicable to geometry. Mass, loads, and restrictions are all discretized in the original continuous mathematical model.

Displacement interpolation functions are a class of polynomial functions that are used to describe the displacement field within the scope of each element and along its sides or edges. The order of the element is determined and specified through the sequence of the displacement interpolation function which is employed in the element. The term "first-order element" is used to refer to an element that employs linear (first-order) displacement interpolation functions. An element is referred to as a "second-order element" in the case it employs second-order displacement interpolation functions, and so on. Displacement arguments Interpolation functions are considered as nodal displacements, and once they are determined, nodal displacements may be used to compute of displacements that exist everywhere in the element. It can be concluded that in the case of it being subjected to a load, this can cause a deformation of the element and it takes on a new shape and also, it will result in each node will move from its original place to a new one. The figure below shows the differences between first-order and second-order elements and their deformation.

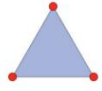
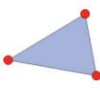
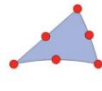
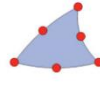
	Before deformation	After deformation
First order		
Second order		

Figure 8 : First-Order and Second-Order Deformation Demonstration [42]

Theoretically, it can be understood that there are an infinite number of methods to mesh a mathematical model for developing a finite element model. A specific mesh can be taken into consideration as a manifestation of a particular discretization decision. The choice of discretization is determined by three key factors, such as the element size, order, and mapping. The relative size of the element is defined by its characteristic dimension. The relative size of the element, in proportion to the dimension of the discretized features, also has a considerable impact. It is generally accepted that an element's size can be approximately estimated by the diameter of the smallest circle that is capable of being inscribed on it. The sequence of displacement interpolation functions is utilized for representing the displacement field within the element itself, along the element edges, and along the element faces to define element order. The element shape functions should be defined before a standard element shape is mapped in order to reflect its true form in the finite-element mesh. This leads to the conclusion that the element form distorts from its ideal shape as a consequence of mapping. In this case, one entity becomes the "master" and the other becomes the "slave" when the displacements of two entities connected to each other.

If a reaction of structure to a load can be completely represented in two dimensions, then 2D components are employed. There are three types of 2D elements called such as axisymmetric, plane stress, and plane strain. Plane stress elements can be expressed as the elements designed in a way to be used in thin, planar constructions that are loaded in a plane, with the out-of-plane stress considered to be equal to zero. Plane strain elements can be described as the elements designed in such a way as to

analyze rigid prismatic structures loaded inside the plane, with out-of-plane strain assumed to be zero. Axisymmetric elements are designed to be used in the study of axisymmetric structures subjected to axisymmetric loads.

Another issue of the FEA design process is the material units. All additional SI units may be easily derived from the three fundamental ones, which are the meter (m), kilogram (kg), and second (s), using the calculation of conversion formulas. In the case of specifying and defining the material properties that are used in FE models and in the case of assigning mass properties to mass elements, paying attention to the importance of the usage of proper units should be taken into consideration. As an illustration, an element having a mass of 1 kg needs to be given a mass of 0.001 tons.

Moreover, the definitions of loads and constraints are included in the boundary condition definitions. Loads are referred to as natural boundary conditions while restrictions are referred to as fundamental boundary conditions in FEA. The gravity or inertial loads are varied by category and can be considered within the category of boundary conditions. Contrary to this, the volume loads do not fall within the category of boundary conditions. Boundary conditions are assigned to geometric entities that exist in a CAD model, and after meshing, these boundary conditions undergo conversion to nodes. It is usually more straightforward to define loads than describe the limitations. Loads are described as vectors identified with direction, sensation, and magnitude such that the latter is quantified. Either the overall load on the mathematical formulation framework or the response forces should be examined in order to confirm the definition of loads. Reaction forces and free-body diagrams, which should always be created prior to analysis, may be compared to ensure that the specification of the constraint is accurate.

In addition to that, in the case of performing a frequency response analysis, it is assumed that the excitation is harmonic, and the magnitude of the excitation depends on frequency rather than time, as it did in a time response analysis.

As a small reminder, Poisson's ratio, which is the negative ratio of transverse to axial strain, and the modulus of elasticity, which defines the link between strain and stress, are considered the only two factors that enable the characterization of a linear

material model. Increasing the amount of stress on the parts in the elastic region also increases the strain linearly. The modulus of elasticity of the part is independent of stress and does not change. The below figure shows that the slope of the stress-strain diagram indicates elasticity.

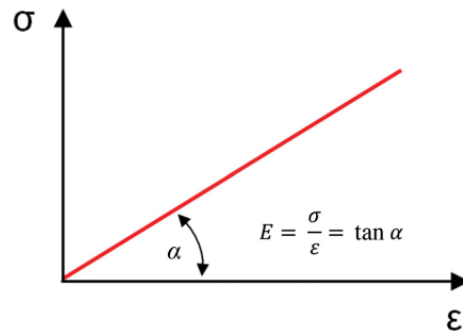


Figure 9 : Stress- Strain Diagram [41]

3.3 Implicit and Explicit Approaches

In numerical analysis methodology, explicit and implicit approaches are utilized to derive numerical approximations in order to solve time-dependent ordinary and partial differential equations that need computer-generated representations of physical processes.

The implicit and explicit methods which are used within the scope of FEM analysis establish the foundation of these solvers. It is important to comprehend differentiations exist between the two numerical techniques during the process of making a determination about which solver to be chosen. At each phase of the solution process for the implicit technique, which is also known as Newton Raphson method, equilibrium between externally applied load and internally produced reaction forces is required. Both incremental and iterative processes are accepted as implicit. Explicit, however, is merely progressive.

While ABAQUS/Standard uses Newton's method, ABAQUS/Explicit uses an explicit central-difference time integration method. [43]

The implicit technique is a widely recognized and renowned for simulating transient problems. The implicit technique has been commonly employed in general simulations due to its benefits in processing speed and numerical precision. One of the most significant characteristics of the implicit method is that it constructs and solves the $Ax=b$ linear algebra equations at each time step. A nonlinear solution, such as a Newton iterative solver, will be used in the case of the governing equation incorporating nonlinear elements. As a result, it can be presumed that the implicit technique is more sophisticated than the explicit technique. Consequently, it requires more computer memory and more intricate software code. Additionally, the concurrent implementation is more difficult. The Newton solver may encounter problems addressing extremely nonlinear models and fail to converge. Due to the fact that the implicit time solvers are unconditionally stable, there is no need to consider numerical stability, and the time step can be adjusted to a bigger value. Furthermore, different residual convergence conditions ensure computational accuracy. It should be considered that when the boundary conditions affect the structure slowly and the effects of strain rates are minimal, implicit techniques should be employed. Once the stress increase as a function of strain has been determined, geometry may be analyzed utilizing implicit techniques. In the model, the global equilibrium is constructed with each time increment. This implies that each increment must converge. After global equilibrium is reached, the solver will be able to compute all of the local finite element variables (stresses, strain, etc.) for each increment.

The explicit technique has a more elementary and simpler methodology compared to the implicit technique. As a result, it does not require the construction of linear algebra matrix equations, thereby eliminating the need to solve a $Ax=b$ linear algebra problem system. It can be concluded that, a nonlinear solver is not required for nonlinear problems, and everything is calculated using a time solver. The explicit technique is more fundamental and simpler to compute, easier to write and implement, and takes up less hardware memory space for processing. Furthermore, the explicit technique offers inherent advantages for parallel processing. It may significantly accelerate parallel processing frameworks like OpenMP, MPI, and GPU. It provides a significant convergence advantage for high-speed, rate-varying problems.

As a disadvantage, it can be given as an example that a small time step must be utilized for fulfilling the numerical stability criterion. Typical explicit solutions include techniques such as the Runge-Kutta methods, the central difference technique, and others.

The explicit analysis techniques should be commenced to be utilized in the case of the strain rates exceeding the value of 10^{-3} per second. For this, these occurrence types of examples such as an automobile accident, a ballistic explosion, a plummet, and so forth can be given. In these circumstances, the rate of strain must be addressed in addition to the variation of stress with strain.

It can be assumed that there are not any iterative processes to be applied or convergence criteria to be evaluated. The solver focuses on calculating local finite element variables. The solver gets obtain results by computing all of the local finite element variables for a specific incrementation before moving on to the next one.

More specifically, the duration value of every step which is used for explicit finite element analysis must be shorter concerning the current time step. Contrary to this, implicit analyses are not constrained in this way. The below figure demonstrates the change of implicit and explicit model graphs according to model size - complexity and efficiency- dynamic.

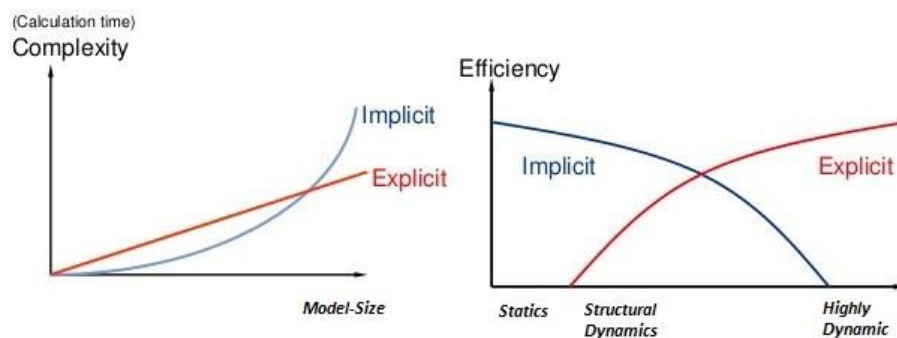


Figure 10 : Complexity and Efficiency for Implicit and Explicit Models [43]

As it is mentioned previously, implicit and explicit techniques can be used within the scope of FEA analysis and the Abaqus tool can be benefited from this type of analysis. Through the utilization of Abaqus tool activities such as conceptual design evaluation, creating design solutions that correspond to the specified requirements and process simulations can be conducted. If it is required to utilize the Abaqus software, different types of solvers are included in it. For example, Abaqus/ Standard solver is available for implicit techniques and Abaqus/ Explicit solver is available for explicit techniques. Abaqus/Explicit solver is utilized for the determination of the solution to a nonlinear problem without iterating by explicitly forwarding the kinematic state from the last increment, but contrary to this, Abaqus/Standard solver must iterate it. Although a specific analysis requires a significant number of iterations through the explicit technique, the evaluation in Abaqus/Explicit solver may be simpler to execute if the equivalent analysis in Abaqus/Standard solver needs many iterations. It can be considered that an additional benefit of the Abaqus/Explicit solver is that it takes substantially less disk space and RAM for the same simulation with respect to Abaqus/Standard solver during the performing of the analysis. For applications where the computational costs of the two systems are equivalent, Abaqus/Explicit solver's significant low disk space usage and memory usage reductions make this solver appealing.[43]

By default, Abaqus/Standard Solver prefers to employ automatic incrementation. To be able to select an acceptable time increment, the rate of convergence is needed to be observed. In the case of only a few iterations are necessary, it is needed to evaluate the increase of the size of the increment. On the contrary, in the case of convergence being evaluated as sluggish, it is needed to consider the reduction of the size of the increment. As another option, in the case of convergence is not achieved, a reduction of the size of the increment is taken into consideration, and further tries are conducted. For smooth nonlinear responses, the implicit method works well. Wrinkling is a buckling interruption that occurs in the nonlinear response. A significant reduction in the magnitude of the time increment may be evaluated as necessary. In rare instances, convergence may be impossible [43].

The explicit method is ideal for high-speed applications. For realistic meshes modeling genuine engineering materials, the constant increment is often minimal. Individual time increments are a low-cost approach. Fine resolutions of fast events can be attained at a cheap cost. Only first-order, reduced integration components can be utilized in general. If continuum components must be utilized to describe bending, this is a serious constraint. Because the approach solves issues by spreading disturbances like waves, it might be incredibly sluggish at first.

3.4 Cohesive Zone Modelling

Before proceeding with the implementation of adhesive joints appropriately and safe manner in engineering applications, it is necessary to conduct a thorough investigation into their mechanical properties. The techniques that benefited from the estimation of the strength of the adhesive joint have made significant progress throughout time. The types of theoretical approaches were initially established utilizing the basic joint geometry. The fundamental target and goal of the theoretical approaches were established to determine the maximum stress values in the adhesive layer and make a comparison between these values and the adhesive strength values. Damage calculations were preferred to be conducted in this manner in accordance with the maximum stress. Numerous numbers of numerical studies which employ the maximum stress/strain approach were carried out over the years subsequent, with the application of the finite element method in the analysis of bonded joints. As a result, through the utilization of the finite element package tools, the stress/strain distributions in the adhesive layer were developed, and damage estimates were carried out by making the comparison between them and the critical values.[44]

Because adhesive joint deterioration is a type of fracture issue, afterward, fracture mechanics techniques were implemented. In the beginning, an extensive range of research studies was carried out with the help of the usage of Linear Elastic Fracture Mechanics. Linear Elastic Fracture Mechanics provides highly accurate outputs and results, particularly in brittle/brittle materials. [45] Studies have been carried out in the Linear Elastic Fracture Mechanics Approach by correlating the loads applied to the

joints with the crack development, stress intensity factor, or energy release rate variables. Although so much work has been done utilizing the Linear Elastic Fracture Mechanics technique, several limits have been found because of the fact that the stress field created at the fracture tip is considered to be totally elastic and plastic deformation is ignored.[46]

New solution approaches have commenced being employed in the mechanical analysis activities of adhesive connections, particularly with the creation of adhesives that have a qualification of high plastic deformation ability and non-brittle qualities. [47] Owing to the fact that the cohesive strength of high-toughness adhesives is closely connected to the plastic area as a result of this constraint in Linear Elastic Fracture Mechanics, investigations on Non-Linear Elastic Fracture Mechanics have been conducted.[48]

The conceptual idea of a cohesive zone had been proposed by researchers in the late 1950s. As a result, stress values observed along a prospective cohesive zone were connected to the reference of the idea of tensile-separation law, and crack propagation experiments and fracture experiments were carried out. [49] As per the developed interface law, the stress levels in the fracture process fluctuate and this fluctuation is determined in accordance with the degree of the deformation. However, at the end of the 1960s, it is devised the J-Integral approach, which can be used on ductile materials, to compute the energy release rate while accounting for plastic deformation at the crack tip. [50] Paid attention was concentrated on the research about the nonlinear fracture behavior of adhesive bonds and those researches were carried out under the direction of these until the 1990s.

The cohesive zone modeling, which is as known as CZM, in particular, made significant progress promptly in the 1990s. Thanks to the increase in the usage of high-toughness adhesives in practice, it becomes more and more crucial than it was ever to investigate the nonlinear fracture behavior of adhesive joints. In light of this, it is clearly understood that the one-parameter, linear elastic fracture mechanics technique is evaluated as insufficient for realistic simulations, particularly in bonding joints created through the help of the usage of the application of high-toughness adhesives. Instead of the single-parameter model utilized in Linear Elastic Fracture Mechanics, it

has been stated that the cohesive region model technique requires two or three parameters for getting obtain more accurate modeling. These criteria can be described such as fracture toughness, cohesive strength, and typical displacement values at which cohesive strength is lost.

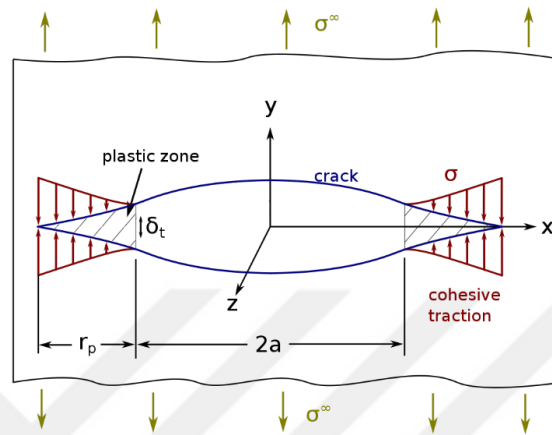


Figure 11 : Cohesive Zone Fracture Model [46]

It is generally contemplated that breakage or delamination occurrences along with the interface, which is prevalent in structures made by mixing materials with various characteristics, such as composites and adhesive joints, have a significantly crucial role in limiting structural strength. This has led to the creation of the possibility of further study on interface damage. Conventionally developed fracture mechanics methodologies can be preferred use for modeling interface separation operations. The cohesive area model approach, which interacts with the fracture mechanism by adopting the traction-separation relations at the interface, has recently been employed as an alternative to classic fracture mechanics techniques. [50] According to the CZM, elastic behavior is displayed up to the peak of the stress-strain curve, and damage commences to emerge at the top of the curve and rupture occurs. Therefore, the substantially vital idea of fracture energy, which is the energy necessary for interface separation, has been developed. In the case of a comparison conducted between the CZM approach and the standard finite element techniques, the CZM approach provides more accurate strength estimates by employing alternative cohesion laws established by taking material and contact factors into account. The CZM approach may simulate

the types of damage development which occur inside the same material as well as at the interfaces of various materials. A group of interface components or contact elements are employed to depict material interfaces so, and the CZM approach is utilized to characterize the interface behavior.

The CZM model is essentially a type of constitutive connection between traction(T) operating on the interface and the associated separation(δ) [51]. The definition of the traction-separation mechanism is determined through the help of either the element type or material model. The CZM approach's shapes such as bilinear, exponential, and trapezoidal are prevalently utilized during the process of the investigation of constructional components.

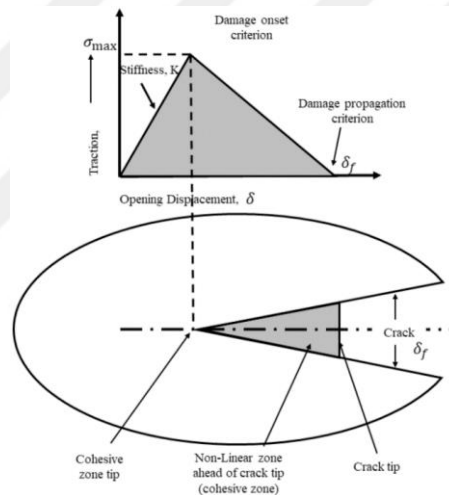


Figure 12 : Traction Displacement Damage Diagram [52]

The CZM approach simulates the elastic behavior up to the maximum stress, which is followed by slow plastic deformation with strength loss and eventual damage. The CZM approach requires the application of traction-separation mechanism rules to the surfaces where separation is predicted.[52] As a result, for tensile and shear circumstances that can occur throughout the fracture path, energy release rate values and critical values or critical toughness values of the applicable material are required. The surfaces where separation is anticipated might be considered within the substance or at the interface of two distinct materials. Normal tensile and shear stress cohesive strengths are end-of-elastic-region properties that should be known.

Abaqus software tool provides a library that is evaluated as considerably beneficial. This library includes information about cohesive components to simulate the reactions of adhesive joints, composite interfaces, and other scenarios where the strength and integrity of interfaces may be important. In order to be able to 2D and 3D fracture analysis, minimum thickness cohesive components are produced. When selecting a Type of Cohesive Element, it comprises two-dimensional (2D), three-dimensional (3D), and axisymmetric (AX) analytical components. COH2D4, for example, is a four-node, two-dimensional cohesive element. The fundamental response of these components is determined by the selection of proper deformation and stress levels for the application region.[53]

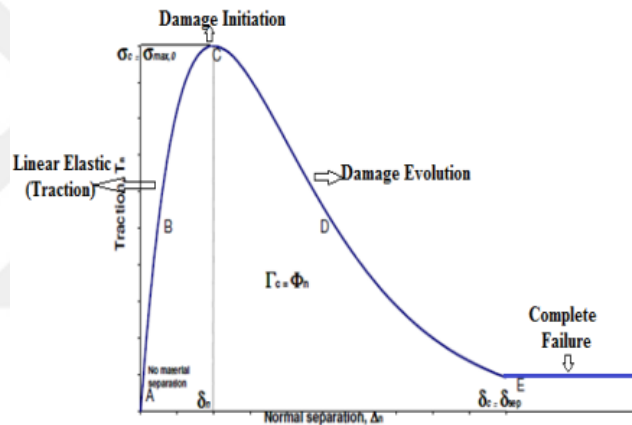


Figure 13 : Separation- Traction Curve [53]

3.5 Validation Part

In order to acquire the qualification to design a suitable harmonic drive, the published work of Yi Cheng Chen and Yun Hao Chang [7], which is related to the study of a harmonic drive with involute profile Flex Spline by two-dimensional finite element analysis, is discussed. The aforementioned study includes both a two-dimensional Harmonic Drive and a related finite element analysis model. By considering the design parameters, the two-dimensional harmonic drive finite element model developed by Cheng has been validated. A total of 30400 elements are utilized within the numerical model of Flex Spline. The number of elements used in the finite

element model is 35158 for the Circular Spline and 629 for the Wave Generator. In accordance with the evaluation results of this reference work, the peak stress value is obtained as 577 MPa at the fillet region and 614 MPa at the contact region under the 50 N.m torque capacity. In parallel, according to the analysis results of thesis obtained in the thesis, the maximum stress in fillet is 567 MPa and the maximum stress in contact is 617 MPa. Consequently, considering the slight difference between the analysis result and the sample data, FEM is suitable for validating sample data. The obtained analysis results and mesh model will be discussed in detail in section 3.5.1.

3.5.1 Analysis of Steel Harmonic Drive

As part of this thesis, the finite element analysis solver of the Abaqus software is utilized for two-dimensional analysis. In the modeling stage of the part, Flex Spline is created as a two-dimensional deformable Shell, and the Wave Generator and Circular Spline are modeled as a two-dimensional Planer Discrete rigid wires considering the design parameters for Harmonic Drive.

The sample article chosen for the review was used for the computation of the Flex Spline geometry. The Flex Spline geometry was divided into different sections, taking into account a uniform mesh distribution and material definitions. The z-axis was used as the symmetry axis in the partitioning of the Flex Spline geometry and the same number of radial pattern, 200, was performed with the number of teeth. During the process of patterning, the rotation angle was set to 360 degrees and this angle was divided by 200 to get 1.8 degrees. By this means, every fragmented region had the same mesh and the same properties.

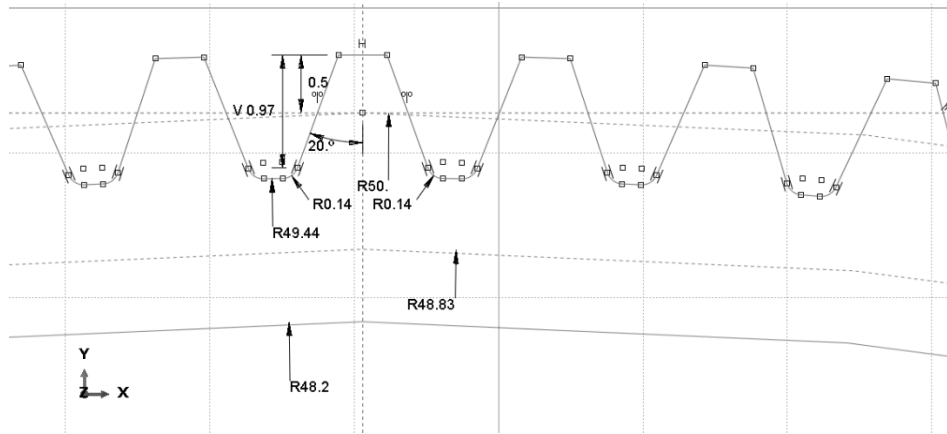


Figure 14 : Sketch of Flex Spline Geometry

The Wave Generator component was designed as a two-dimensional discrete rigid wire part. The assumption that the Wave Generator is too rigid to be deformed in the analysis, led to rigid modeling of Wave Generator. For this reason, the stresses that occur in the Flex Spline will be negligibly higher. The geometric dimensions of the Wave Generator were determined according to the sample article. The minor radius of the Wave Generator with the elliptically shape was calculated to be 47.575 mm, whereas the major radius was 48.825 mm.

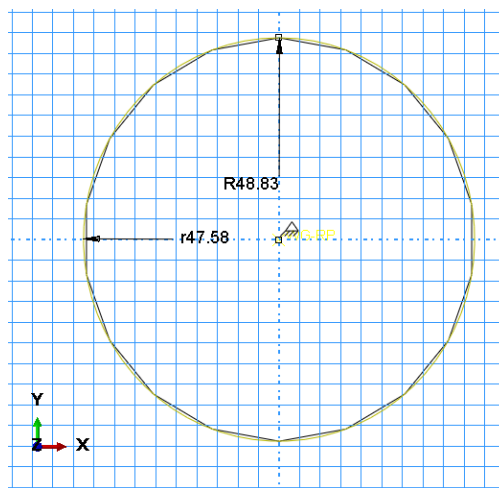


Figure 15 : Sketch of Wave Generator Geometry

Similar to the Wave Generator, the Circular Spline component is designed as a two-dimensional discrete rigid wire. The value of pitch diameter (101 mm) was multiplied by the total number of the Circular Spline teeth(202) and the tooth modulus of the Circular Spline(0.5 mm) was obtained. Only some of the teeth of the Flex Spline and Circular Spline will be exposed to contact with each other during the shrink fit, and the torque will be transmitted through them.

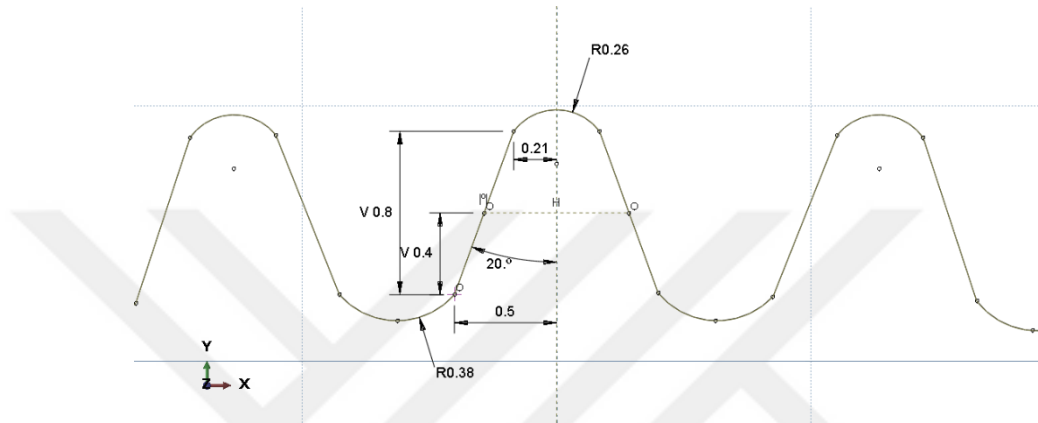


Figure 16 : Sketch of Circular Spline Geometry

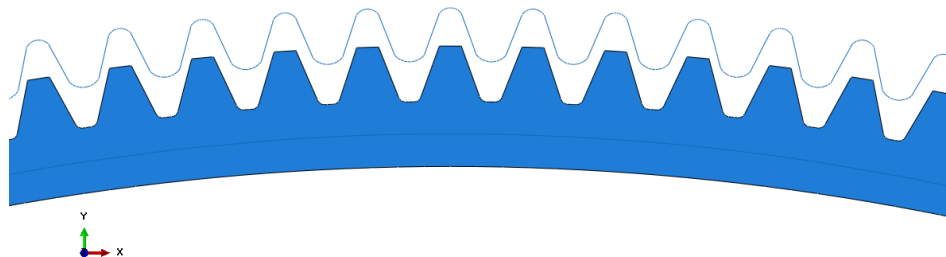


Figure 17 : Assembly sketch of Harmonic Drive

In finite element analysis, it is important and necessary to accurately determine the mechanical properties and attributes of the parts. For steel materials, the reference work material was utilized [7], where Young's modulus of the steel material is defined as 200 GPa, and Poisson's ratio is taken as 0.29 in the calculations. In addition, in order to examine whether the part has a plastic deformation, stress-plastic strain relationship is shown in Table 3.1.

Table 3. 1 : Plastic elongation of steel due to stress [7]

Yield Stress [MPa]	Plastic Strain
860 MPa	0.000
950 MPa	0.035
1000 MPa	0.045
1050 MPa	0.075
1080 MPa	0.085

After the material definitions, section definitions should be conducted in Abaqus software. The suitable section is constructed as the solid, homogeneous type for the steel regions.

For the Harmonic Drive's assembly group, three components are gathered under the assembly and positioned properly. In the positioning operation, the major axes of the three components are overlapped and the teeth of the Flex Spline and the Circular Spline are aligned to mate with each other at the interference step.

The first step of the analysis algorithm was described as the interference step. At the interference step, the Wave Generator causes deformation in the Flex Spline and forms it into an elliptical geometry. At the end of the interference step, the pressure occurs in the inner surfaces of the Flex Spline and the stresses occur in the different sections of the Flex Spline. This step was created as a general static step, which means the operation will take place in small steps and dynamic effects will not occur where the period was selected as 1 second and the increment size was defined as 0.00001 seconds.

The second step of the analysis algorithm can be described as the torque step. During this torque step, the Wave Generator rotates around the major axis, while the Circular Spline remains stationary, and the torque is applied to the Flex Spline. The other parameters, such as time period, increment size, and solution technique, were similar to the interference step.

In the analysis, the interactions between the surfaces described previously should be arranged according to the steps. Two interactions were defined within this scope. The first interaction occurs between the Flex Spline and the Wave Generator, while the second interaction occurs between the Flex Spline and the Circular Spline. Furthermore, three constraints were defined for each component that needs to be controlled.

The interaction defined between the Flex Spline and the Circular Spline is established during the torque step. At the point of the interaction which occurs between the teeth sections of the Flex Spline and the Circular Spline, the surface of the Circular Spline is designated as the master, while the surface of the Flex Spline is designated as the slave.

The boundary conditions and the loads need to be defined, propagated or adjusted in other steps. It should be noted that there is only one component to which the load is applied, which is the reference point of the Flex Spline. This reference point controls the inner surface of the Flex Spline through a coupling interaction. The applied torque magnitude was defined as 50 N.m in the counter-clockwise direction. Regarding the boundary conditions of the harmonic drive components, as shown in Figure 18, Flex Spline is fixed at the rotation of Z, free in X and Y directions during the initial step and interference step. In the torque step, the Flex Spline is free at the rotation of Z, and its displacement is set to 0 mm in X and Y directions. During the initial step and interference step, the reference point, which controls the surface of the Wave Generator through a coupling interaction, is fixed in X, and Y directions as well as the rotation of Z direction. In the torque step, the rotation of Z is set to 6.28 rad, and the displacement in X and Y directions is set to 0 mm. Circular Spline is fully fixed in each step.

Components	Directions	Steps		
		Initial	Interference	Torque
Flex Spline	X	Free	Free	0
	Y	Free	Free	0
	rotation of Z	Fixed	0	Free
Wave Generator	X	Fixed	0	0
	Y	Fixed	0	0
	rotation of Z	Fixed	0	6,28
Circular Spline	X	Encastré		
	Y			
	rotation of Z			

Figure 18 : Boundary conditions of Harmonic Drive components at each step

Last but not least, the meshing operation is considered one of the most significant processes that directly impacts on the outcomes of the analysis where very large or very small mesh size will cause different errors in the results. For this reason, a coarse mesh is preferred for the regions, and mesh sensitivity analyses were conducted to reduce the mesh size in critical regions until a suitable outcome was reached. Since the Flex Spline is the most critical part, more seeds were assigned to the contact and the fillet zones. In other words, it is presumed that the contact and the fillet regions require a finer mesh, while the remaining regions can have a coarser mesh. In addition, the element type was chosen the 4-node bilinear plain strain quadrilateral with reduced integration (CPE4R). Both the Wave Generator and the Circular Spline had the same seeding methodology. The seeds were assigned both to the surface of the Flex Spline and to the surface of the Circular Spline with 0.05 mm intervals. The element type was selected to be a 2-node 2-D linear rigid link (R2D2) for use in plane strain (or plane stress) for both components. In the Flex Spline finite element model, a total number of 98800 elements were employed. Moreover, the total number of 23018 elements for the Circular Spline and the total number of 1514 elements for the Wave Generator were employed in the model. Table 3.2 provides a comparison between the number of elements in the sample data and the finite element model. Also, Table 3.3 presents the number of seed in Flex Spline mesh model.

Table 3.2 : The number of elements in sample data and FEM results

	Sample Data	FEM
Wave Generator	629	1514
Flex Spline	30400	98800
Circular Spline	35158	23018

Table 3.3 : The number of seeds in Flex Spline

Surfaces	Quantity of Seed
Tooth Face	29
Fillet	7
Horizontal Curves	11
Vertical Lines	9

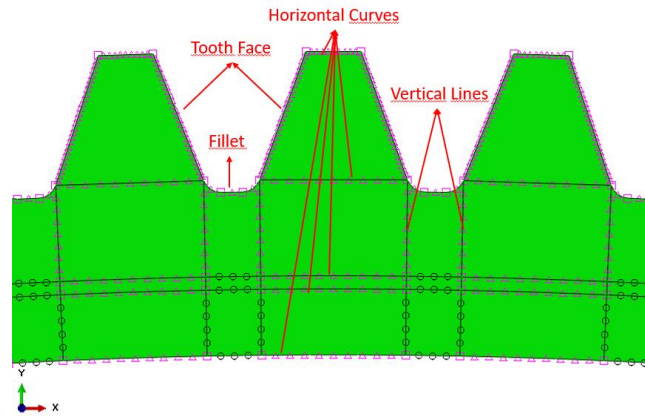


Figure 19: Applied Seed Distribution to Flex Spline

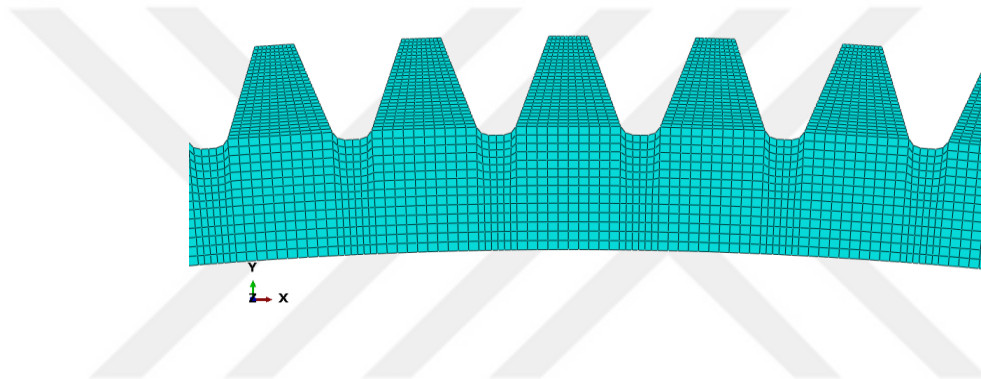


Figure 20: Mesh Distribution on Flex Spline

As a result of the analysis, it has been determined that when a magnitude of 50 N.m of torque is applied to the Flex Spline, the maximum observed von Mises stress is 617 MPa, which occurs at the contact region between the Flex Spline and the Circular Spline. On the other hand, the maximum observed von Mises stress in the fillet region is calculated as 567 MPa. When comparing the analysis results to the sample data, the subsequent conclusions make sense, the error in the maximum von Mises stress occurring in the contact region is approximately 0.5 percent, and the error in the maximum von Mises stress in the fillet region is around 1.8 percent. As a consequence, it has been verified that the analytical model and the mesh structures in the numerical model are appropriate enough.

3.5.2 Hybrid Design

In this section of the study, the hybrid harmonic drive gear design is discussed in order to increase torque capacity while reducing the weight, and a finite element model was developed. While creating the finite element model, the geometric dimensioning of the Flex Spline was not altered in order to ensure reasonable comparisons with the geometry of the steel Flex Spline. In the hybrid Harmonic Drive design, the factors such as composite material, adhesive material, the directional orientation of material, the cohesive zone model, meshing element type, and cross-sectional areas of materials are discussed.

As a beginning, the carbon fiber and the glass fiber materials have been selected, and those materials are assigned to the composite region of the Flex Spline. Due to the fact that the composite materials do not behave isotropically unlike the steel material, the properties of the materials can be different according to the directions. For this reason, the carbon fiber and the glass fiber materials are defined as shown in Table 2.2 and Table 2.3 in order to fully reflect the behavior of the parts. The hybrid Harmonic Drive design requires an adhesive to bond the composite and steel regions together and epoxy-based Araldite adhesive was selected for this purpose.

Regarding the hybrid harmonic drive, the inner side of the Flex Spline was modeled as 0.5 mm in thickness carbon fiber materials and the composite section was bounded to a steel section with 0.1 mm in thickness adhesive material. The steel material was assigned for the remaining regions including the Flex Spline threads. Owing to the fact that the directional mechanical behavior of the material varies for composite materials, the material orientation was developed in this section. It was expected that the Flex Spline would carry the load according to the direction where the maximum load will be applied.

In the hybrid Harmonic Drive design, another issue to be looked into is delamination. In order for the delamination to be examined, a cohesive zone modeling (CZM) was created. and the element type of the region was changed to a 4 node of two-dimensional cohesive element (COH2D4). Steel, adhesive, and composite in Figure 21 are demonstrated with green, pink, and yellow respectively.

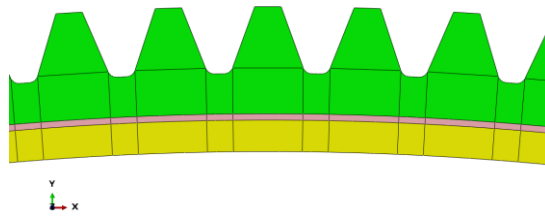


Figure 21 : Section Demonstration of Hybrid Flex Spline



CHAPTER 4

RESULTS AND DISCUSSIONS

In this section, the findings of the analysis of the steel Flex Spline will be shared and explained. In addition, the results obtained from the improvements in the hybrid Harmonic Drive design will be examined. Tensile stress, elastic deformation, plastic deformation, delamination, and torque capacity will be discussed for different conditions. Also, natural frequency parameters of steel and hybrid Flex Splines' will be compared to evaluate the effect of vibration.

4.1 Steel Flex Spline Analysis

In this section, the comparisons between mesh and stress values are made based on the assumption that the mesh structure in the sample work is appropriate.

4.1.1 Mesh Sensitivity

Mesh sensitivity analysis is a method of approaching more accurate results in stress by iteratively increasing the number of mesh elements. Analysis results become more stabilized as the mesh approaches from coarse to fine mesh. As the number of elements used in the analysis increases, the analysis will take longer because the number of equations that the solver program has to solve increases. In addition, another important parameter in mesh sensitivity analysis is solution time. Therefore, when the analysis results stabilize, the number of elements is not increased considering the solution time and the mesh is considered fine. Within the scope of this thesis, it is aimed to find the number of elements that will provide the reference article's stress values in critical regions by accepting the stress values shared in the sample article as accurate enough.

In the sample article, when a torque of 50 N.m is applied to the Flex Spline, the von Mises maximum stresses of 614 MPa and 577 MPa were found in the contact and fillet regions, respectively. In this context, mesh density in the contact and fillet regions

of the Flex Spline plays a critical role. First, as shown in Figure 22, 15 seeds were placed on the fillet region and 10 seeds were placed on the tooth face with 5 biases towards the center. The maximum von Mises stress obtained in this mesh structure is 435 MPa in the contact region and 650 MPa in the fillet region. The stress value is high because the dimensions of the elements in the fillet region are very small, and the stress value is low because the size of the elements in the contact region is very large. In the figures of stress analysis results, the location of maximum contact stress is demonstrated on “C” point, and “F” refers to the location of maximum fillet stress of Flex Spline.

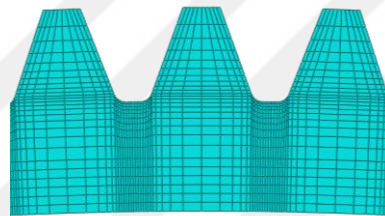


Figure 22 : First Mesh Structure of Flex Spline Geometry

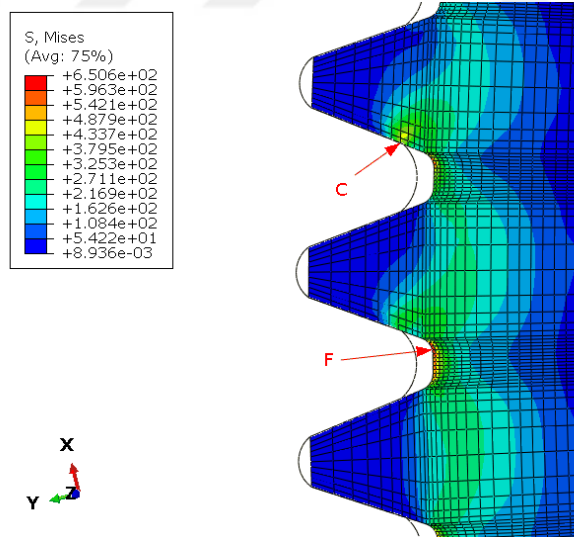


Figure 23 : Stress Analysis Results of Steel Flex Spline with First Mesh Structure

Considering the stress values in the sample article, the number of seeds in the fillet area was decreased, the number of seeds on the tooth surface was increased and the mesh structure of the Flex Spline shown in Figure 24 was created. In the new mesh

model, there are 7 seeds in the fillet area, while there are 19 seeds on the tooth surface. The results of the analysis in Figure 25 showed that the stress value in the fillet region was close to the target value, the stress value in the fillet region was 567 MPa and the stress value in the contact region was 479 MPa which is below the compared value.

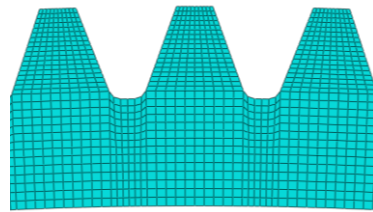


Figure 24 : Second Mesh Structure of Flex Spline Geometry

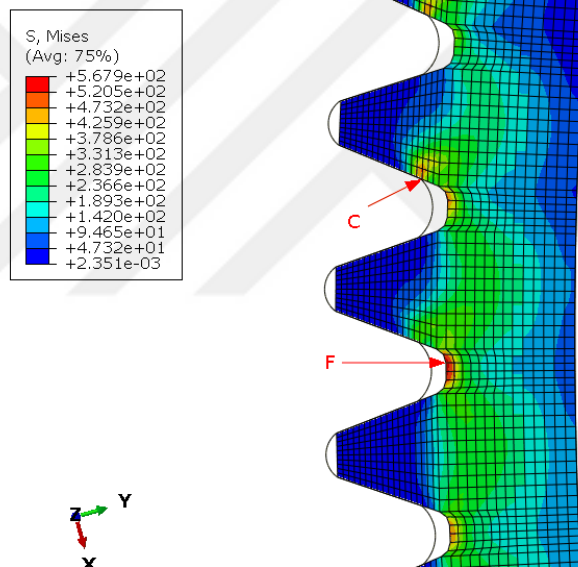


Figure 25 : Stress Analysis Results of Steel Flex Spline with Second Mesh Structure

In order to verify the maximum stress value in the contact area, which is a critical area, the number of seeds in the tooth surface in these areas was increased to 27. The new mesh model created is shown in Figure 26, the stress in the contact region is 617 MPa and the strain in the fillet region is 567 MPa. By looking at the obtained stress values, In addition, the second-order was selected in the mesh element type in Figure 28 and the result of the reanalysis was obtained. As a result, the maximum von Mises stress was found to be 616 MPa. This result shows that the element size is

appropriate. It can be said that the mesh model can be accepted for analysis according to the analysis results of the new mesh model shown in Figure 27.

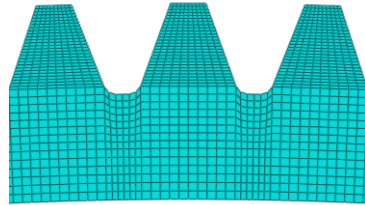


Figure 26: Third Mesh Structure of Flex Spline Geometry

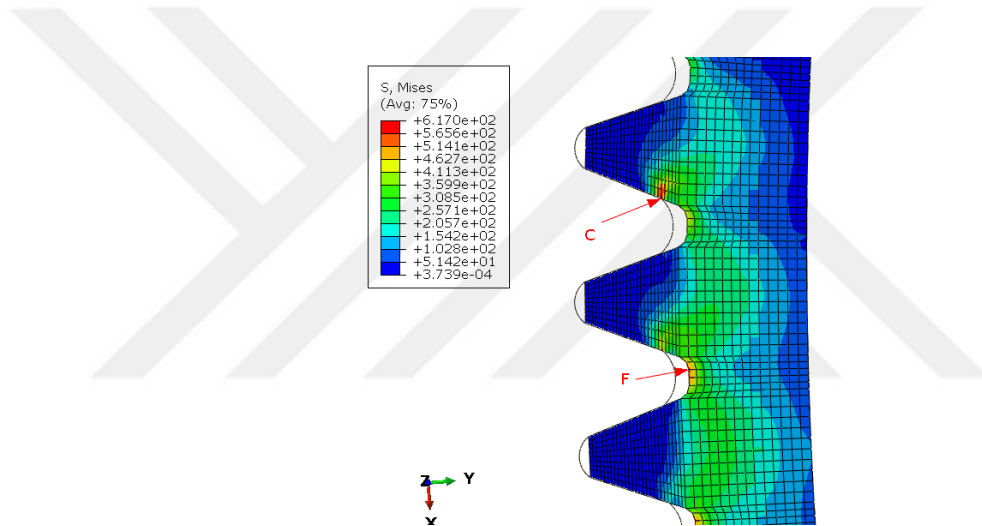


Figure 27 : Stress Analysis Results of Steel Flex Spline with Third Mesh Structure

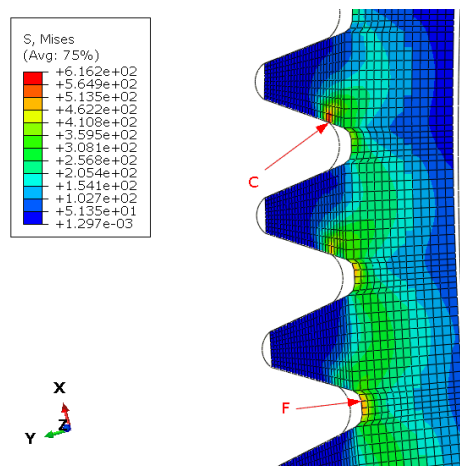


Figure 28 : Stress Analysis Results of Steel Flex Spline with Second- Order Accuracy of Third Mesh Structure

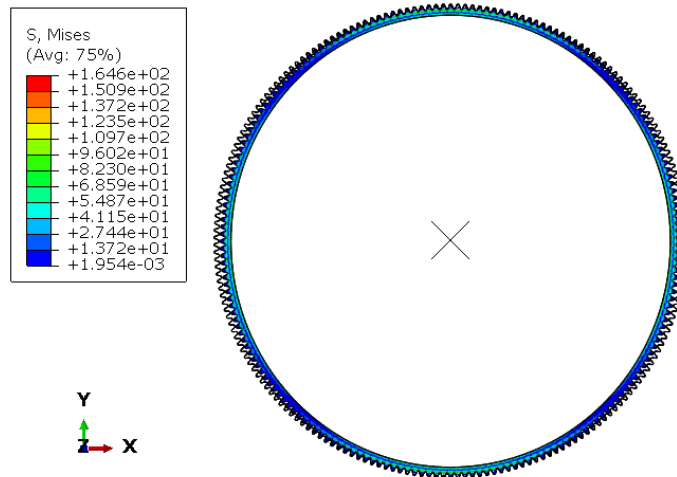


Figure 30 : Harmonic Drive Assembly at the end of the Interference Step

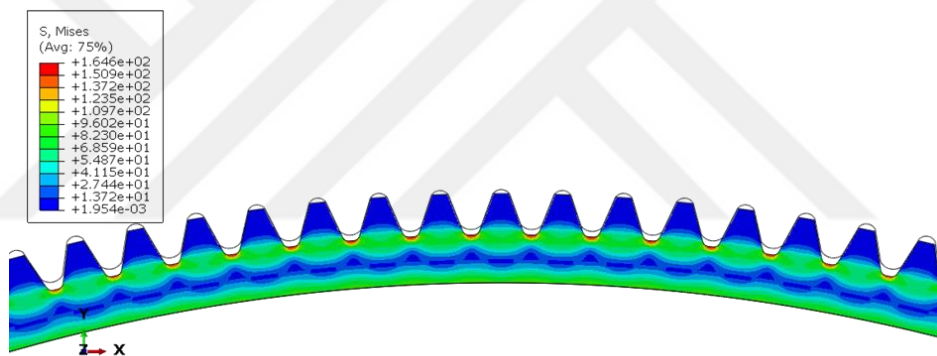


Figure 31 : Stresses on Steel Flex Spline at the end of the Interference Step

In the torque application step, while the Wave Generator rotates 720 degrees counterclockwise, the Circular Spline is fixed and a torque of 50 N.m is applied to the Flex Spline from the reference point. The stresses occurring on the Flex Spline are shown in Figure 33 and also, and Figure 32 shows the Harmonic Drive assembly at the end of the torque step. In this step, the maximum stress on the Flex Spline occurs in the Flex Spline and Circular Spline contact regions with a magnitude of 617 MPa. Also, the maximum stress on the fillet region is 567 MPa. When the analysis findings are compared to the sample article, there is a 0.5 % error in the maximum von Mises stress happening in the contact area and a 1.8 % error in the highest von Mises stress

occurring in the fillet region. Given the relatively low error in stresses, the Flex Spline design is considered verified.

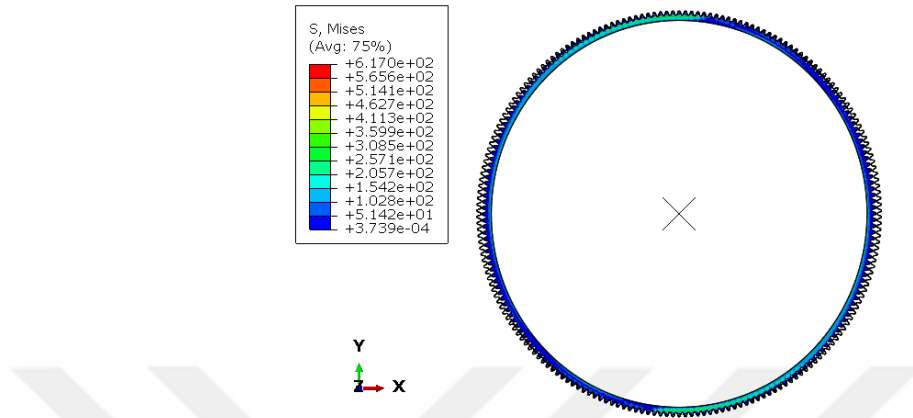


Figure 32 : Harmonic Drive Assembly at the end of the Torque Step

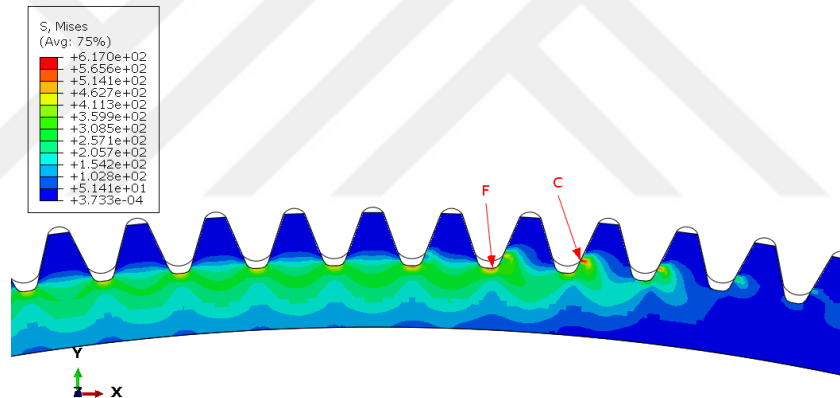


Figure 33 : Stresses on Steel Flex Spline at the end of the Torque Step

Strain values in Flex Spline are shown in Figure 34. Similarly, in regions with high-stress values, strain values were also high. According to the results of the analysis, the largest strain value was 0.002924 in the fillet region.

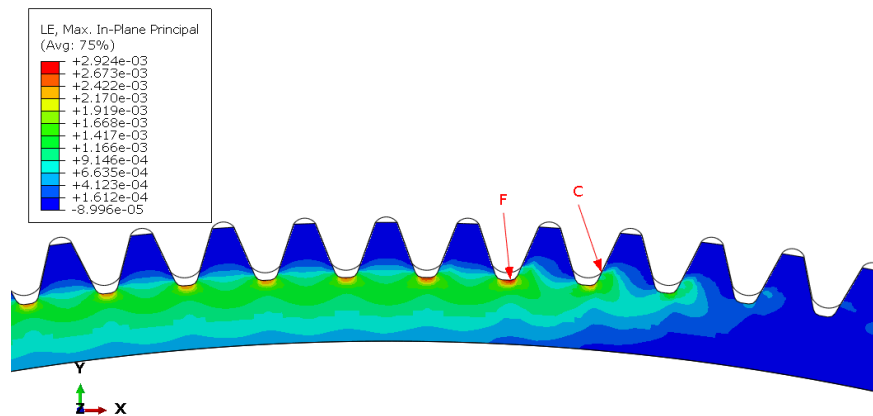


Figure 34 : Strain on Steel Flex Spline

Figure 35 is shared to examine the plastic deformations that occur in the Flex Spline. As seen in Figure 35, the plastic deformation in all elements on the Flex Spline is 0. When the stresses formed on the Flex Spline are examined, it is seen that the yield stress limit of 860 MPa has not been exceeded. For this reason, plastic deformation does not occur in Flex Spline.

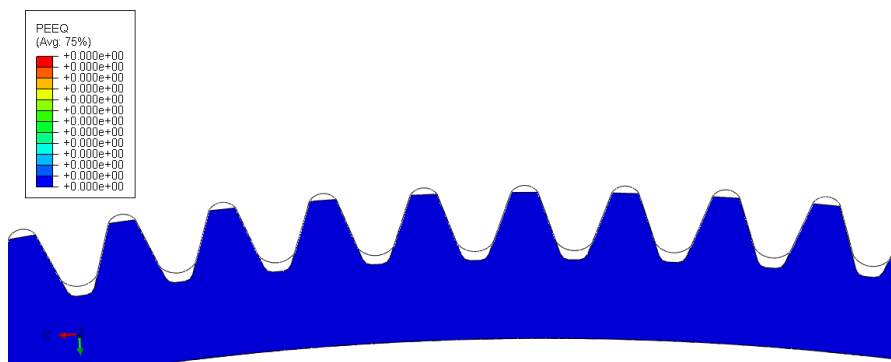


Figure 35 : Plastic Deformation Demonstration of Steel Flex Spline

The variation of the stresses occurring in the “C” point of the Flex Spline over time is shown in Figure 36, and the variation of the stresses occurring in the F node of the Flex Spline over time is shown in Figure 37. As can be seen from the graphs, the stresses in the contact and fillet regions increase in certain time intervals and then

decrease. Similar to Figure 36, Figure 38 shows the variation of forces in the contact zone with time. The forces peak when the teeth come into contact with each other and then become 0.

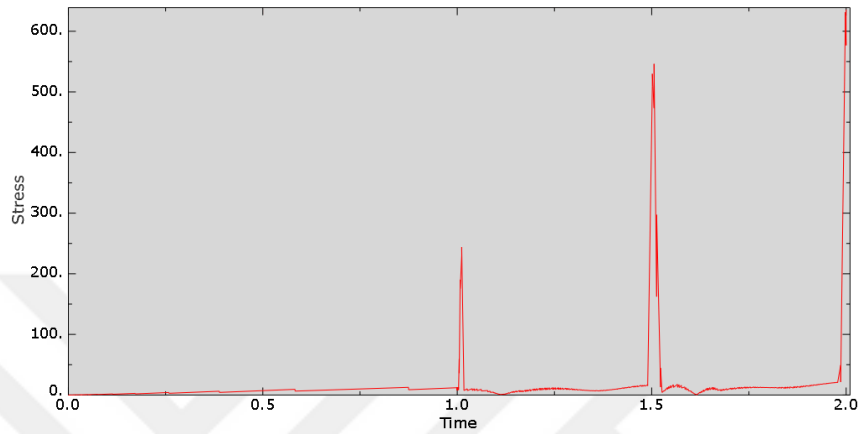


Figure 36 : Variation of Stresses Occurring on the “C” point of Steel Flex Spline

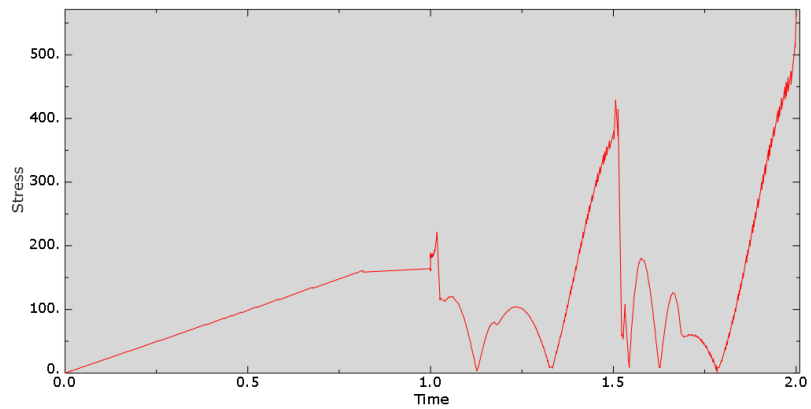


Figure 37 : Variation of Stresses Occurring on the “F” point of Steel Flex Spline

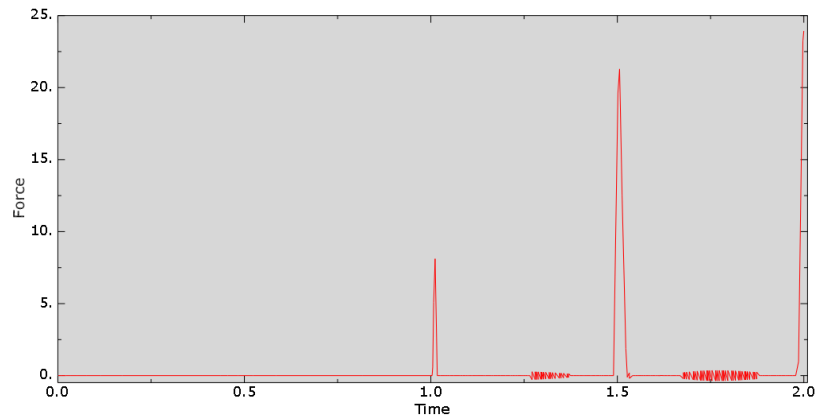


Figure 38 : Variation of Forces Occurring on the “C” point of Steel Flex Spline

4.2 Hybrid Flex Spline Analysis

As previously stated in the hybrid design, the hybrid Harmonic Drive was modeled as 0.5 mm thick carbon fiber, 0.1 thickness mm adhesive, and the rest of it steel material (0.64 mm). In Figure 39, the maximum von Mises stress in a hybrid Harmonic Drive is shown. In steel Flex Spline, the maximum von Mises stress occurs in the contact region, while in this hybrid Flex Spline model, the maximum von Mises stress which occurred in the fillet region is 633 MPa. In Figure 40, Strain values in hybrid Flex Spline are shown. Where the maximum stress occurs, the maximum strain has occurred and its value is 0.00336. In this hybrid Flex Spline model, the stress and strain values increased slightly. On the other hand, almost half of the rim thickness is designed using composite material instead of steel material. This change makes a significant difference in the weight of the Flex Spline. However, von Mises stress and strain values of Flex Spline geometry including 0.5 mm thickness Carbon fiber composite and 0.1 mm thickness adhesive resin have higher values compared to steel Flex Spline.

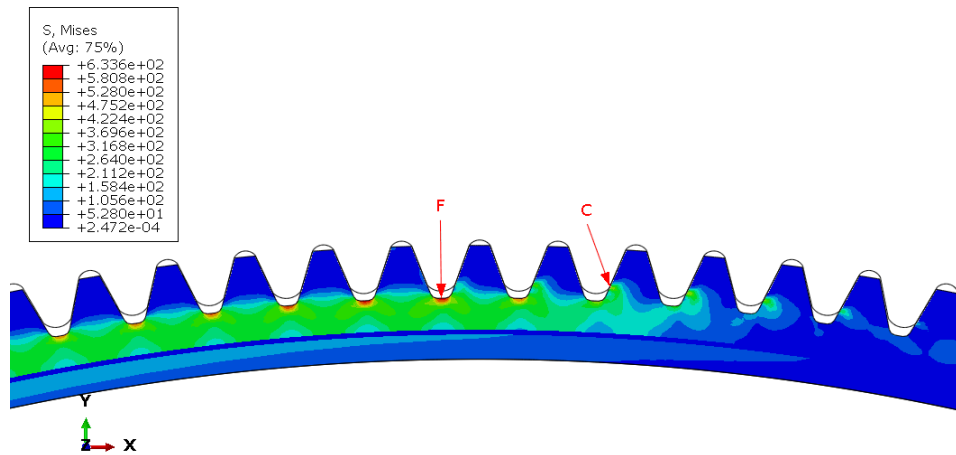


Figure 39 : Stresses on Hybrid Flex Spline with Carbon Fiber at the end of the Torque Step

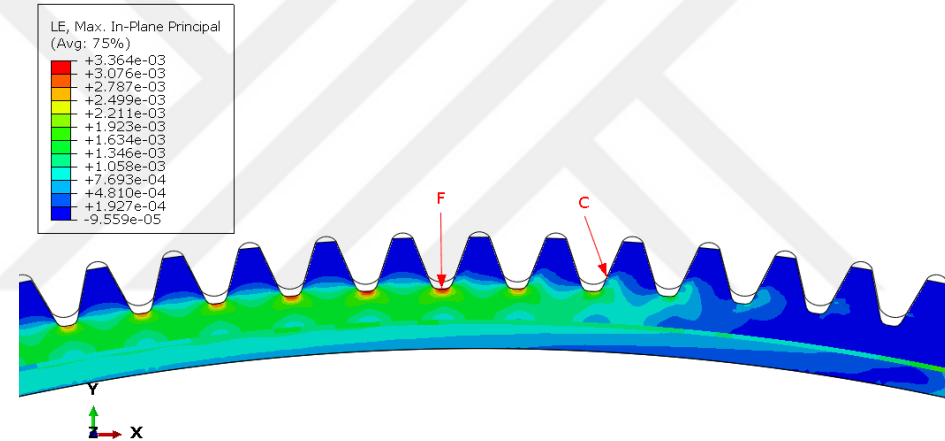


Figure 40 : Strain on Hybrid Flex Spline with Carbon Fiber

By examining the stress distribution in the hybrid Flex Spline model, it can be said that plastic deformation does not occur because the maximum von Mises stress does not exceed the yield stress which is 860 MPa for steel and 1200 MPa for composite. As can be seen in Figure 41, plastic deformations in Flex Spline were investigated and it was shown that there was no plastic deformation.

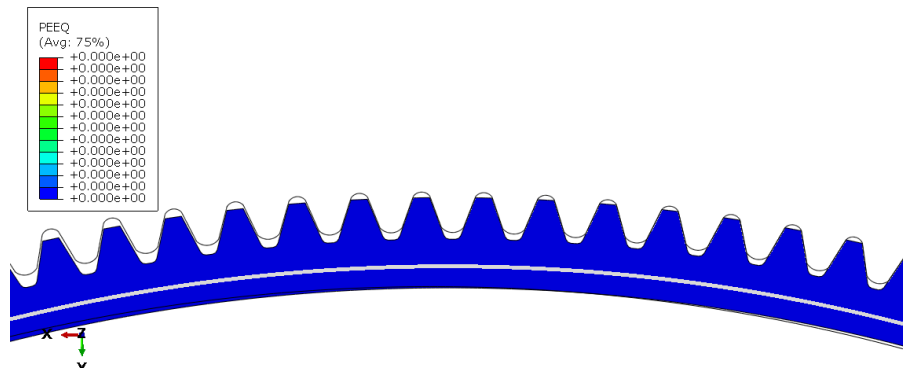


Figure 41: Plastic Deformation Demonstration of Hybrid Flex Spline with Carbon Fiber

The variation of the stresses occurring in the F node of the hybrid Flex Spline over time is shown in Figure 42, and the variation of the strain due to the stress is shown in Figure 43.

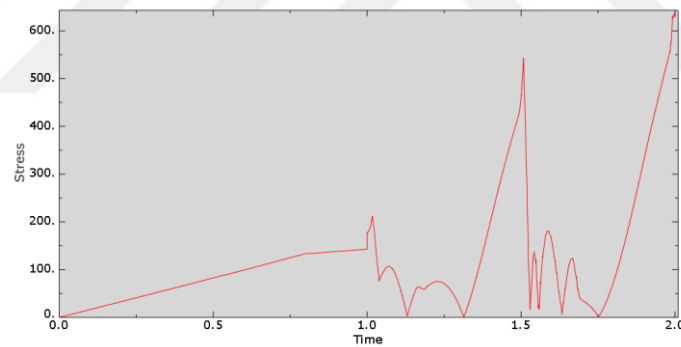


Figure 42 : Variation of Stresses Occurring on the “F” point for Hybrid Flex Spline with Carbon Fiber

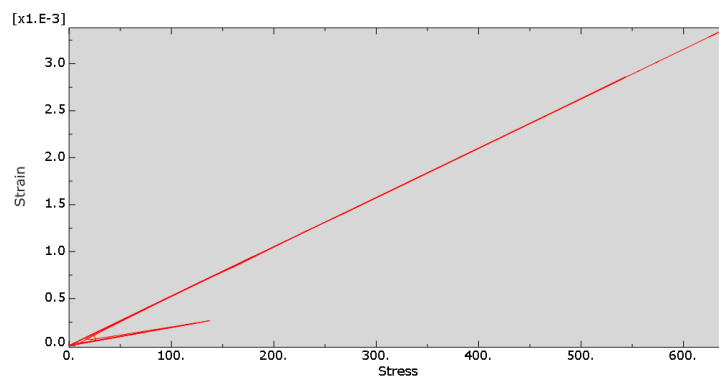


Figure 43 : Stress-Strain Graph for Hybrid Flex Spline with Carbon Fiber

Another issue examined in the hybrid Flex Spline model is delamination, which indicates whether there is a crack in the bonded interface. According to Figure 44, no delamination occurs on the part. In the case of delamination, the adhesive material and the composite material are separated from each other and cracks that will occur in the composite part can be observed depending on time. In Extended Finite Element Method (XFEM) analysis, elements, where cracks start, are indicated in red. In XFEM analysis, the absence of cracks indicates that the design is suitable under the specified conditions.

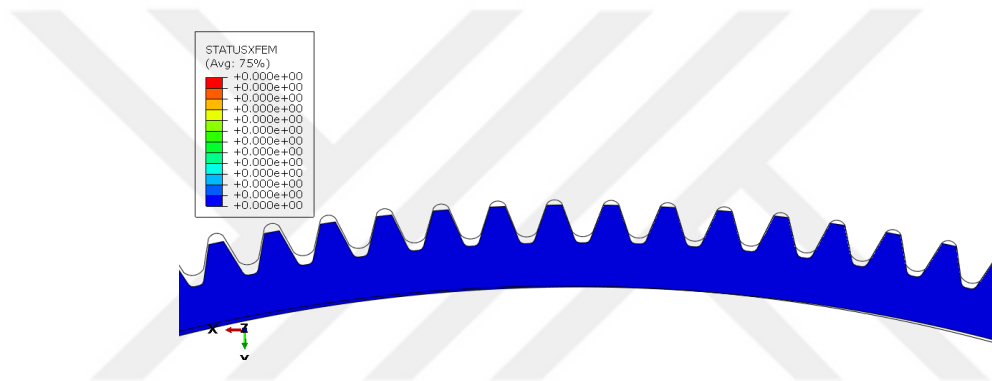


Figure 44 : Delamination Representation of Hybrid Flex Spline with Carbon Fiber

4.2.1 Design Optimization

In this part of the thesis, alternative hybrid harmonic drive designs were considered. First, it was observed how the analysis result was affected when the material of the adhesive used in the design was changed. Epoxy resin Araldite LY3505/XB3405 with a young module of 3.5 GPa was used instead of epoxy adhesive Araldite 2015 with a young module of 1.8 GPa. When the results of the analysis were examined, no change was observed in the stresses occurring in the Flex Spline. After replacing the adhesive material, the maximum stress in Flex Spline was observed to be 637 MPa. Based on this, it can be said that the effect of the adhesive material on the torque capacity and weight is negligible.

In order to examine the effect of replacing the composite material, glass fiber composite material was defined instead of carbon fiber. The defined glass fiber is assigned to the composite region. The stresses in the new hybrid Flex Spline under the effect of 50 N.m of torque are shown in Figure 45. According to the results of the analysis, the maximum stress of 641 MPa, which exceeds the fatigue strength, occurs in the fillet region, and also, the maximum strain value of Glass Fiber – Steel Flex Spline is 0.003843. Therefore, it is clearly seen that glass fiber exerts stress values higher than carbon fiber in the “F” points.

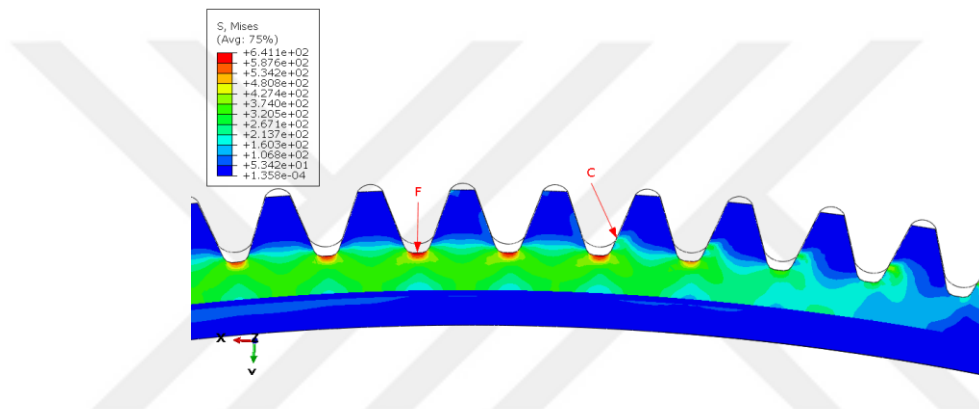


Figure 45 : Stresses on Hybrid Flex Spline with Glass Fiber at the end of the Torque Step

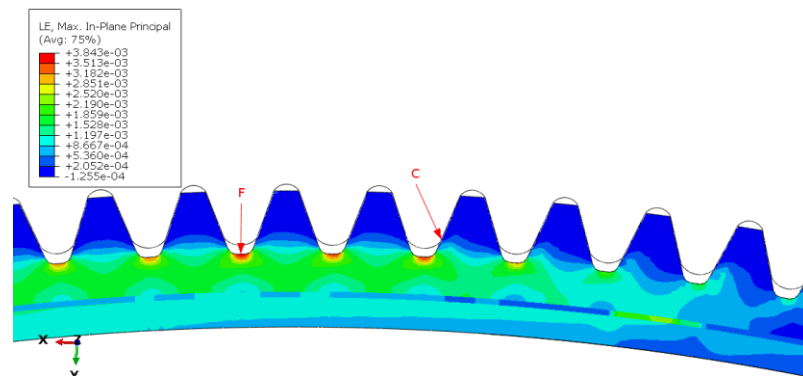


Figure 46 : Strain on Hybrid Flex Spline with Glass Fiber

Another parameter was reducing the thickness of the adhesive material and increasing the thickness of the steel in the reduced region. In this context, the adhesive thickness was reduced from 0.1 mm to 0.05 mm and then to 0.01 mm. In contrast, the maximum stresses in the hybrid Flex Spline decreased from 637 MPa to 610 MPa and

592 MPa, respectively. Based on this, as can be seen in Figure 47 and Figure 48, changing the adhesive material did not change the stresses, while reducing the thickness of the adhesive material and increasing the thickness of the steel zone by an equal amount reduced the stresses significantly. In addition, if the strain values shown in Figure 40 and Figure 49 are compared, it was observed that the maximum strain value decreased from 0.00336 to 0.00286 by decreasing the adhesive resin thickness from 0.1 mm to 0.01 mm.

Normally, due to the ductile nature of the adhesive material, it is expected to increase the elasticity of the system and decrease the stress values that will occur. Based on this, the stresses should increase as the thickness of the adhesive material decreases. However, since the adhesive used in the thesis was brittle, it was observed that when the thickness of the material was reduced from 0.1 mm to 0.01 mm, the stress decreased from 637 MPa to 592 MPa.

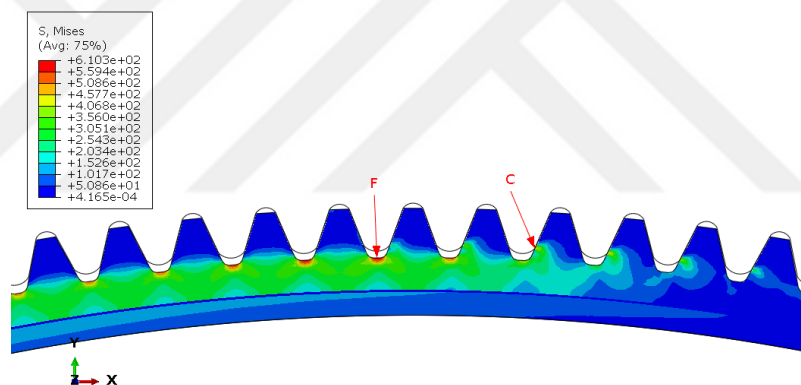


Figure 47 : Stresses on Hybrid Flex Spline with 0.05 mm Adhesive Resin

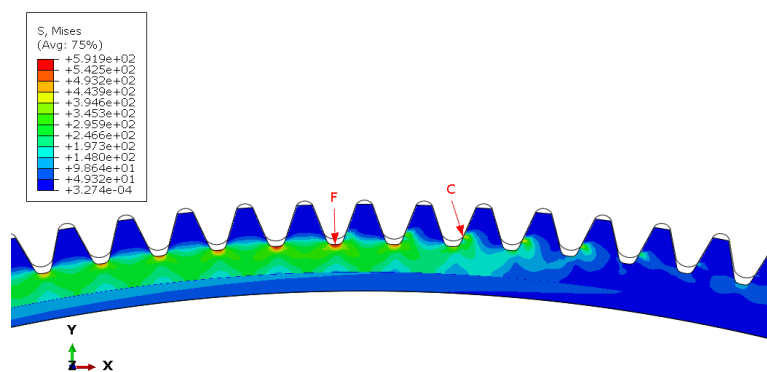


Figure 48 : Stresses on Hybrid Flex Spline with 0.01 mm Adhesive Resin

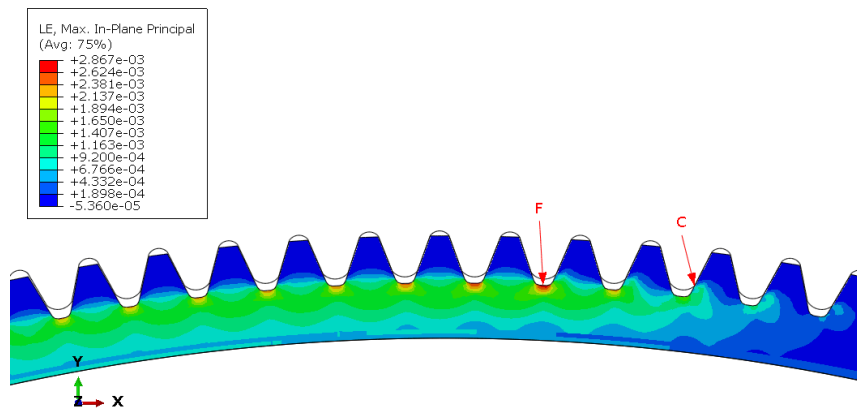


Figure 49 : Strains on Hybrid Flex Spline with 0.01 mm Adhesive Resin

The next parameter to be examined is the thickness of the composite material. Flex Spline models with 0.4 mm, 0.3 mm, 0.2 mm, and 0.1 mm composite thickness were designed by decreasing the thickness of the carbon fiber model by 0.5 mm thickness by 0.1 mm. The von Mises stress distributions formed in the models are shared in Figure 50, Figure 51, Figure 52, and Figure 53, respectively.

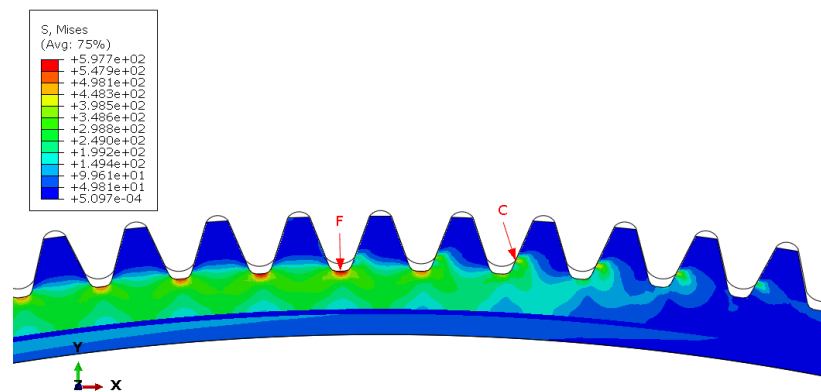


Figure 50 : Stresses on Hybrid Flex Spline with 0.4 mm Carbon Fiber

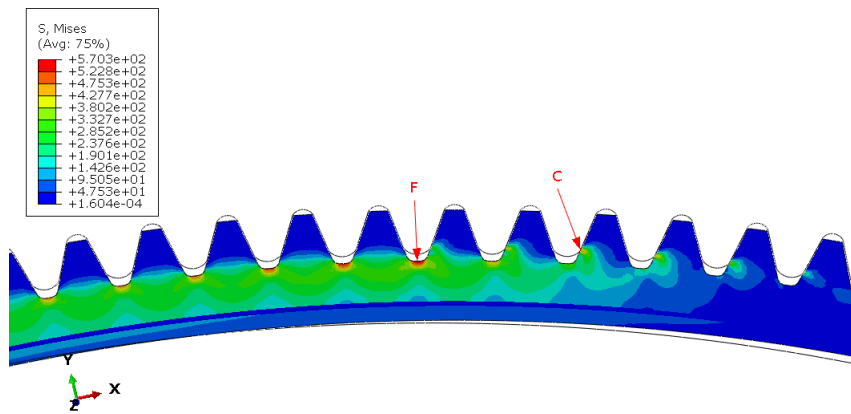


Figure 51 : Stresses on Hybrid Flex Spline with 0.3 mm Carbon Fiber

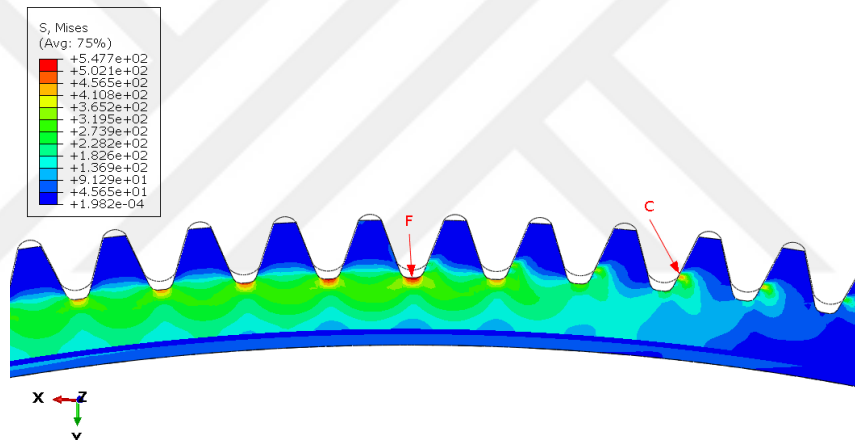


Figure 52 : Stresses on Hybrid Flex Spline with 0.2 mm Carbon Fiber

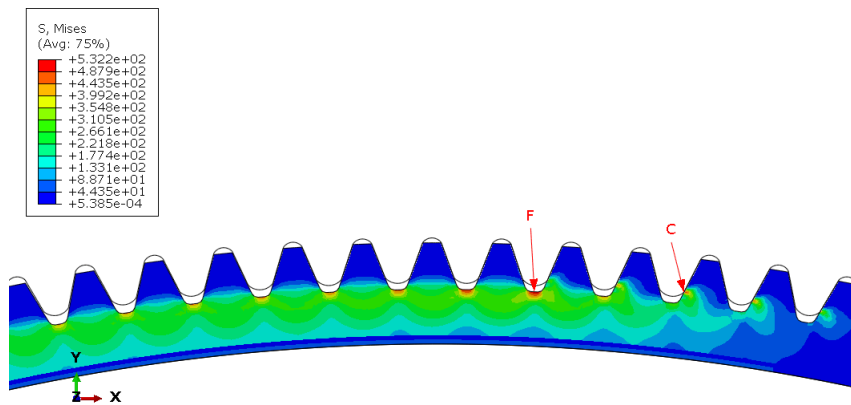


Figure 53: Stresses on Hybrid Flex Spline with 0.1 mm Carbon Fiber

The stress values under 50 N.m torque of the hybrid Harmonic Drive models, obtained by reducing the thickness of the composite region of the Flex Spline by 0.1 mm, are shared in Figure 54. As shown in Figure 54, the von Mises stresses visibly decreased when the thickness of the composite region was decreased and the steel region was increased. Thanks to this improvement, hybrid Flex Spline models have moved away from the fatigue strength limit and the amount of applicable torque has increased gradually for these designs.

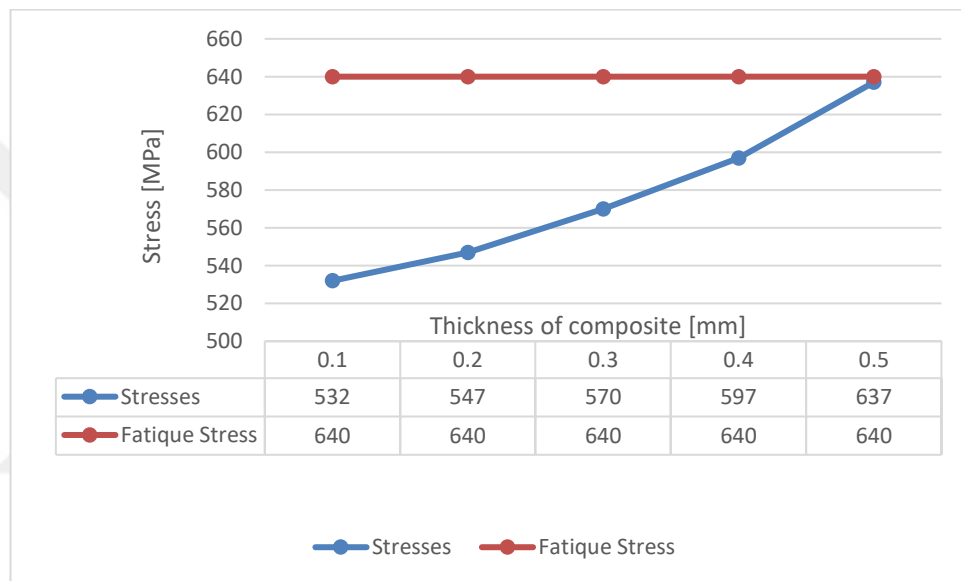


Figure 54 : Maximum Stresses and Fatigue Strength Limit in Hybrid Flex Spline at Different Composite Thicknesses

50 Nm, 60 Nm, 65 Nm, 70 Nm, and 75 Nm torques were applied to find out how much the torque capacity of the hybrid harmonic drive with a composite section thickness of 0.1 mm increased. As shared in Figure 55, the stresses obtained according to the applied torque values were found to be 532 MPa, 607 MPa, 618 MPa, 627 MPa, and 642 MPa, respectively. Based on the results, if 0.1 mm carbon fiber and 0.1 mm adhesive are used in the designed harmonic drive, an increase of around 20 N.m is achieved in the torque capacity of the harmonic drive. This increase has been evaluated in a way that the stresses that will be created by the applied torque do not exceed the fatigue strength, that is, the endless usage situation.

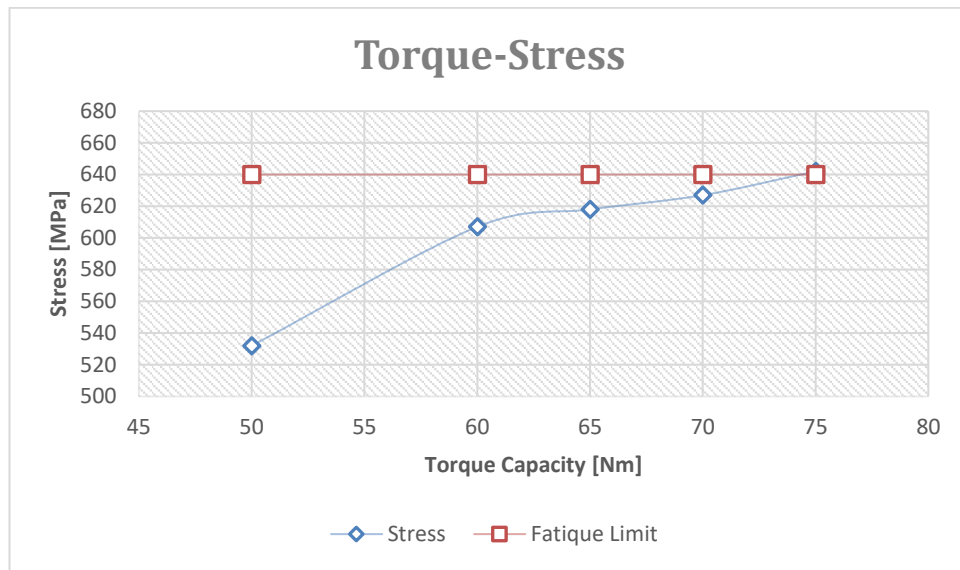


Figure 55 : Maximum Stresses and Fatigue Strength Limit in Hybrid Flex Spline with 0.1 mm Composite Thickness Under Different Torques

4.2.1.1 Additional Composite Reinforcement Comparison Part

In another hybrid harmonic drive design, instead of reducing the steel section and adding composite, the steel section was kept constant and 0.3 mm carbon fiber composite was added with 0.1 mm adhesive. In this design, the Circular spline has not been changed and the major and minor radii of the Wave Generator have been reduced. In the new Wave Generator design, a minor radius of 47.175 mm major radius of 48.425 mm were calculated by subtracting 0.4 mm. As shown in Figure 56, the maximum von Mises stress in hybrid Flex Spline is 573 MPa in the fillet region and 549 MPa in the contact region. While the maximum stress was 617 MPa in steel the Flex Spline, the maximum stress decreased to 573 MPa when 0.1 mm adhesive and 0.3 mm composite were added to the steel Flex spline. In this design, while the use of additional material in the section area increases the weight, the natural frequency has increased as will be explained in the 4.2.1.4 section. In addition, an increase in torque capacity will occur thanks to the reduction of stresses.

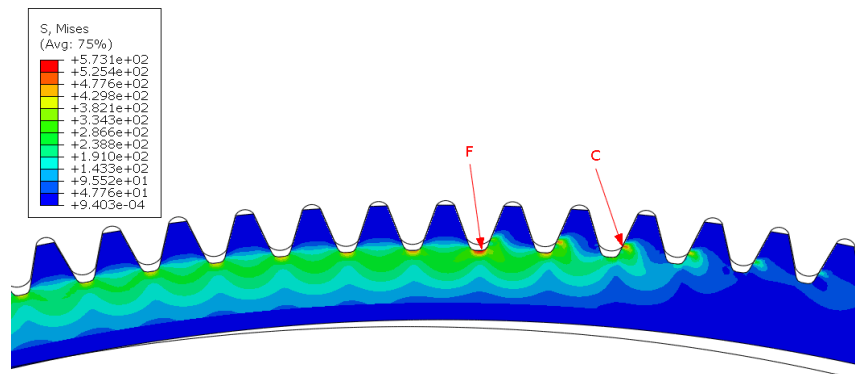


Figure 56 : Maximum Stresses of Steel Flex Spline with Additional Composite Reinforcement

4.2.1.2 Contact Force

When a torque of 50 N.m is applied to steel Flex Spline and Hybrid Flex Spline with 0.1 mm Carbon Fiber, the forces generated in the contact areas when the Flex Spline-Wave Generator and Flex Spline-Circular Spline surfaces come into contact are shared in Figure 57 and Figure 58. In this interaction, the greatest contact force occurs between Flex Spline and Circular Spline. This value was 53 N for the steel flex spline whose rim thickness is 1.24 mm and decreased to 47 N for 1.04 mm steel, 0.1 mm adhesive, and 0.1 mm carbon fiber the hybrid Flex Spline. In addition, the Flex Spline with Additional Composite Reinforcement with 1.24 mm steel, 0.1 mm adhesive, and 0.3 mm composite were included in the examination of the forces generated at the contact. It was observed that the maximum force formed at the contact between the additional composite reinforced Flex spline and the Circular spline was 50 N as shown in Figure 59. On the hybrid Flex Spline designs, the contact force between Flex Spline and Circular Spline master-slave surfaces has decreased as a result of this trial.

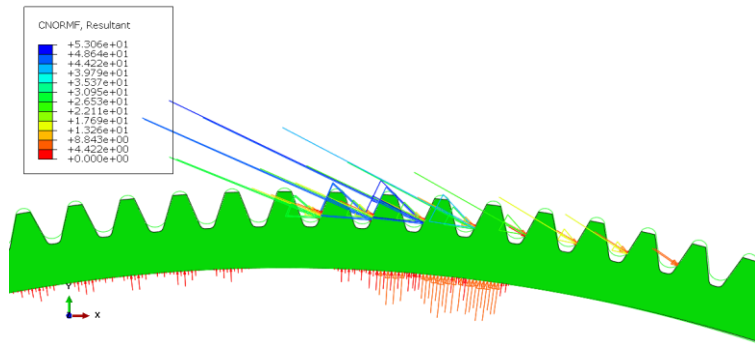


Figure 57 : Contact Force Between Contacting Surfaces in Circular Spline and Steel Flex Spline

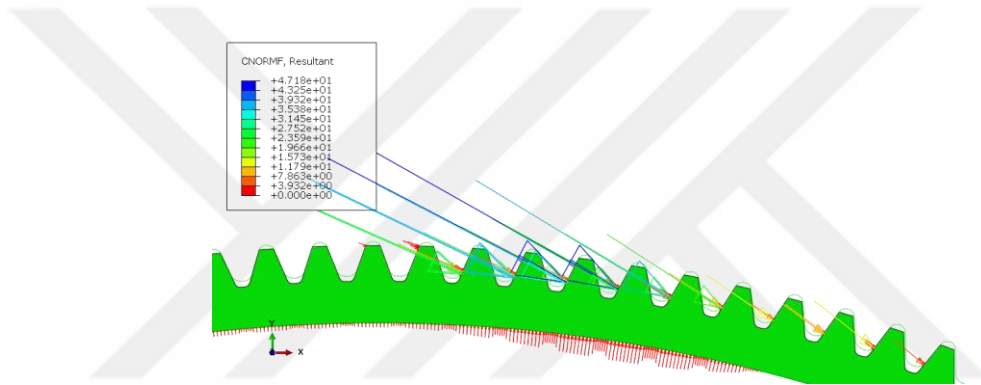


Figure 58 : Contact Force between Contacting Surfaces in Circular Spline and Hybrid Flex Spline with 1.04 mm Steel, 0.1 mm Adhesive and 0.1 mm Carbon Fiber

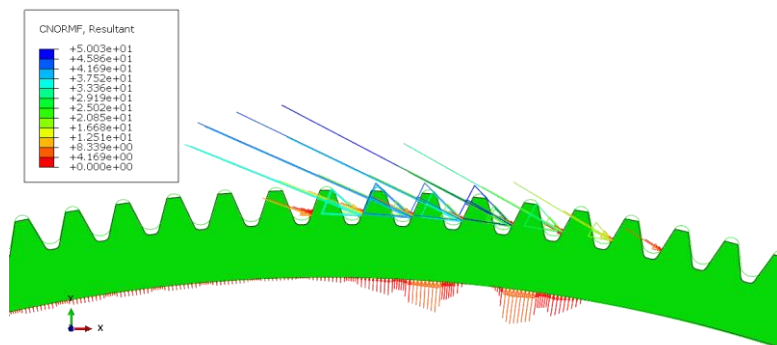


Figure 59 : Contact Force between Contacting Surfaces in Circular Spline and the Flex Spline with Additional Composite Reinforcement

4.2.1.3 Mass Reduction Comparison Part

Alongside stress reduction and torque capacity enhancement optimization for the Hybrid Harmonic Drive, weight reductions for the hybrid harmonic drives under investigation are also discussed. In the weight reduction calculations, the rim thickness section of Flex Spline was evaluated and the weight was correlated with the density per unit area. In the hybrid flex spline design, the weight of the designs is noticeably reduced compared to the steel Flex Spline, as the composite is much lighter than steel. In the calculations, the individual areas of the sections to which the material is assigned were calculated as in Table 4.1 and the values as in Table 4.2 were obtained by multiplying by the density of the material to be assigned. The amount of reduction of the resulting weight values relative to the steel flex spline is shared proportionally in Table 4.3. According to the composite thickness used, the rim thickness section weight can be reduced up to 38.35 percent among the optimized hybrid Flex Splines.

Table 4. 1 : Rim Thickness Section Areas of the Optimized Flex Splines

Area [mm ²]				
Flex Spline Model	Steel Section	Adhesive Section	Composite Section	Total
124	380,39mm ²	0	0	380,39mm ²
104-01-01	319,69mm ²	30,38mm ²	30,32mm ²	380,39mm ²
94-01-02	289,25mm ²	30,44mm ²	60,70mm ²	380,39mm ²
84-01-03	258,74mm ²	30,51mm ²	91,14mm ²	380,39mm ²
74-01-04	228,17mm ²	30,57mm ²	121,65mm ²	380,39mm ²
64-01-05	197,54mm ²	30,63mm ²	152,22mm ²	380,39mm ²
124-01-03	380,39mm ²	30,26mm ²	90,39mm ²	501,03mm ²

Table 4. 2 : Rim Thickness Section Mass of the Optimized Flex Splines

Mass [gr/mm]				
Flex Spline Model	Steel Section	Adhesive Section	Composite Section	Total
124	2,97 gr/mm	0 gr/mm	0	2,97 gr/mm
104-01-01	2,49 gr/mm	0,04 gr/mm	0,05 gr/mm	2,58 gr/mm
94-01-02	2,26 gr/mm	0,04 gr/mm	0,10 gr/mm	2,39 gr/mm
84-01-03	2,02 gr/mm	0,04 gr/mm	0,15 gr/mm	2,20 gr/mm
74-01-04	1,78 gr/mm	0,04 gr/mm	0,19 gr/mm	2,01 gr/mm
64-01-05	1,54 gr/mm	0,04 gr/mm	0,24 gr/mm	1,82 gr/mm
124-01-03	2,97 gr/mm	0,04 gr/mm	0,14 gr/mm	3,15 gr/mm

Table 4. 3 : Mass Reduction on Optimized Flex Splines

Flex Spline Model	Reduction Rate
124	-
104-01-01	12,99
94-01-02	19,35
84-01-03	25,73
74-01-04	32,12
64-01-05	38,52
124-01-03	-6,20

4.2.1.4 Natural Frequency

Natural frequencies are present in all physical formations. When the structure is exposed to specific external stresses, these frequencies have a tendency to vibrate. “The distribution of mass and stiffness inside the structure affects these frequencies [54]”. In order to find the natural frequencies, the density information of the materials must be defined. The density of steel is taken as 7.8 g/cm³, The density of carbon fiber is defined as 1.6 g/cm³, and the density of adhesive was selected as 1.3 g/cm³. In theory, steel should have a lower natural frequency than composite because of elasticity and density. Considering working speed, flexspline may be exposed to resonance. One way to avoid resonance is to change the natural frequency of the flex spline. The study examined the natural frequency of Flex Spline. Only the first mode of the Flex Spline was investigated in the Harmonic Drive design, because the output speed varies from 20 rpm to 500 rpm. For full steel modeling, the first frequency has produced 717 cycle/time values as shown in Figure 60. Secondly, the full composite modeling first mode 1048 cycle/time result was produced as in Figure 61. The initial mode is 563 cycle/time if the steel material is subtracted by 0.6 mm, 0.1 mm of which is defined as adhesive resin and 0.5 mm as composite material shared in Figure 62. However, the mode is 845 cycle/time if the steel material thickness of the Flex Spline component is raised from 1.24 mm to 1.64 mm, so 0.3 mm composite material and 0.1 mm adhesive resin are added to the steel material. The results of the final analysis are also shown in Figure 63. As a consequence, it has been observed that when steel is reinforced with composite material, the natural frequency increases; but, when composite material is added by reducing the steel material, the natural frequency might decrease. It is not possible to say which harmonic drive is more suitable because the

operating speed of the flex spline is unknown. Given that steel HD has a natural frequency of 717 rpm and hybrid flex with composite reinforcement has a natural frequency of 845 rpm, it can be assumed that if the flex spline operating speed were 300 rpm, hybrid flex with composite reinforcement would produce less vibration because it moves away from a resonance zone.

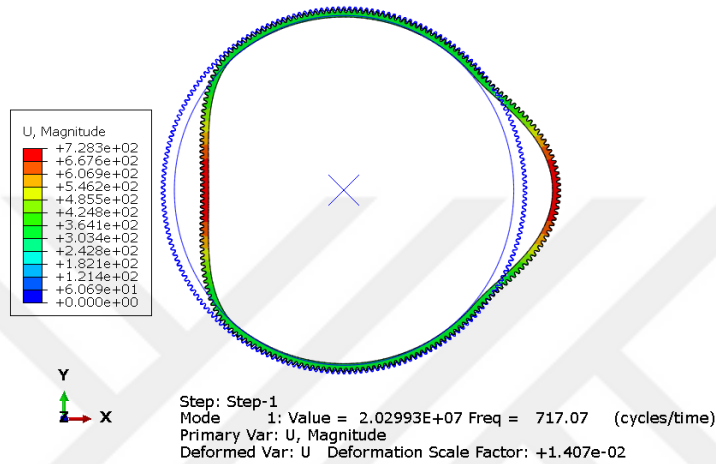


Figure 60 : First Mode of Steel Flex Spline

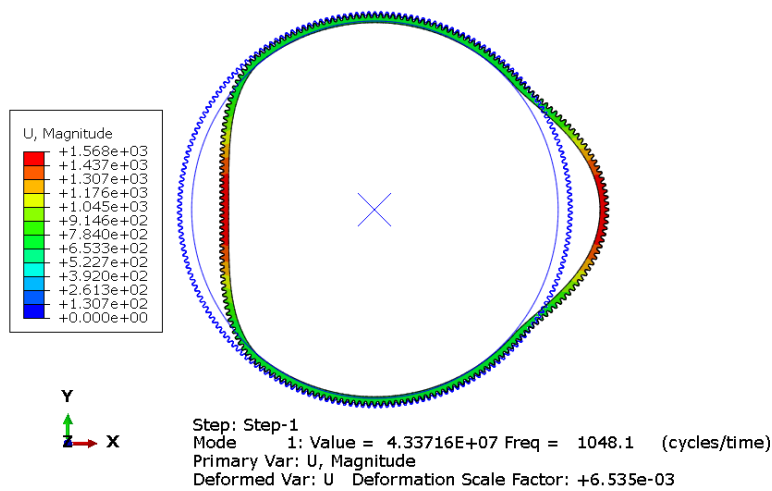


Figure 61 : First Mode of Carbon Fiber Flex Spline

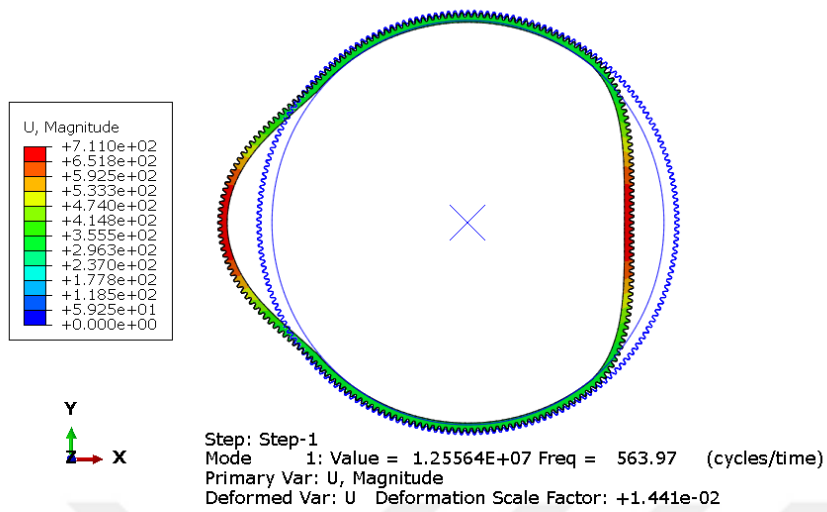


Figure 62 : First Mode of Flex Spline when Rim Section is 0.64 mm Steel, 0.1 mm adhesive and 0.5 mm Carbon fiber

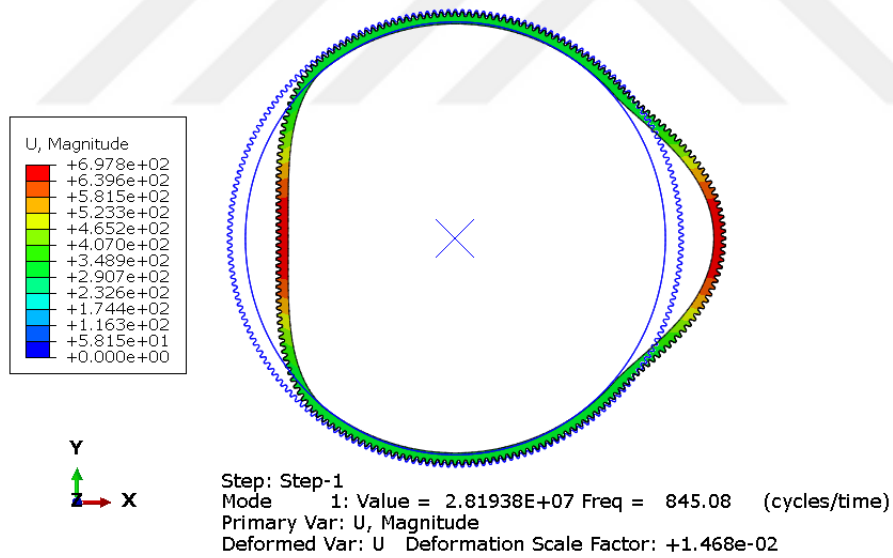


Figure 63 : First Mode of Flex Spline when Rim Section is 1.24 mm Steel, 0.1 mm adhesive and 0.3 mm Carbon fiber.

CHAPTER 5

CONCLUSION

Harmonic drive, which is a strain wave gear, has been used in many application areas in recent years. The fact that technology for designing and producing such gear systems has not yet been developed extensively.

In spite of the fact that Harmonic Drive has provided an extensive number of advantages, it has some disadvantages as well. A great deal of researchers have been proceeding with their studies in order for improving the Harmonic Drive technology. It has been known that Harmonic Drive is composed of three different components such as the Flex Spline, the Wave Generator, and the Circular Spline. The fluctuation and vibration problem is counted as one of the disadvantages of the Harmonic Drive technology and some studies have been conducted to find out a solution to this problem. For transmitting the motion appropriately and correctly, the Flex Spline is required to be flexible in the radial direction, notwithstanding, to be stiff in the torsional direction. In a great number of studies, it is shown that this component which is manufactured from steel material, can be made of anisotropic material, to increase the capacity of damping. Within the scope of this study, with the utilization of composite materials, it has been aimed to reduce both the von Mises stress, and the weight of the component and at the same time to increase the value of the torque capacity.

This study has commenced with the design stage of the Harmonic Drive geometry which is taken from the sample work and the results of stresses demonstrated in this work have been utilized for the validation stage of the numerical analysis model. The maximum von Mises stress in the contact area and the highest von Mises stress in the fillet region differ by 0.5% and 1.8%, respectively, when the analytical results are compared to the sample article.

It was observed that the use of carbon fiber composite material for the hybrid Flex Spline has reduced the value of stress to a lower level concerning the glass fiber material.

The effects of adhesive type are seen to be negligible. However, it can be underlined that the reduction of the thickness of the adhesive resin decreased the stress values, because mechanical behavior of the adhesive resin materials was brittle.

The use of the steel material which is reinforced with the composite material and reducing the thickness of the steel material by less than 0.4 mm have reduced the von Mises stress values compared to the full steel model. Thereby, it can be concluded that the applicable torque capacity has been increased thanks to the reduced stress values.

The contact forces in the Circular Spline have reduced in the hybrid Flex Spline concerning the steel Flex Spline. Furthermore, the natural frequency of the system was increased without subtracting the steel thickness of Flex Spline. This is an achievement for avoiding the resonance zone and reducing vibration while taking into account the operational range.

Finally, torque capacity increased by about 27.7 % while stress values, contact force, and weight have decreased by 13.7 %, 11.3 %, and 38,5 % respectively thanks to the different Hybrid Flex Spline designs.

5.1 Future Work

Given the conclusions of my investigation, as a concept of future study, the gear profile can be applied to the hybrid Flex Spline. Furthermore, the torsional angle and correspondingly the torsional stiffness study may be conducted. Most importantly, the validation of the composite flex Spline analyses can be conducted using appropriate experimental works.

REFERENCES

- [1]. Majchrak, M., et al. "Analysis of harmonic gearbox tooth contact pressure." IOP Conference Series: Materials Science and Engineering. Vol. 659. No. 1. IOP Publishing, 2019.
- [2]. Kiyosawa Y., Takizawa N., Ohkura T., Yamamoto Y., *A New Strain Wave Gearing*, JSME, 23-26 November 1991, 1132-6.
- [3]. Tuttle, Timothy Douglas. *Understanding and modeling the behavior of a harmonic drive gear transmission*. Diss. Massachusetts Institute of Technology, 1992.
- [4]. Nye, Ted W., and Robert P. Kraml. "Harmonic drive gear error: Characterization and compensation for precision pointing and tracking." *JPL, The 25th Aerospace Mechanisms Symposium*. 1991.
- [5]. Kayabasi, Oguz, and Fehmi Erzincanli. "Shape optimization of tooth profile of a flexspline for a harmonic drive by finite element modelling." *Materials & design* 28.2 (2007): 441-447.
- [6]. Ostapski, W. "Analysis of the stress state in the harmonic drive generator-flexspline system in relation to selected structural parameters and manufacturing deviations." *Bulletin of the Polish Academy of Sciences: Technical Sciences* (2010): 683-698.
- [7]. Chen, Yi-Cheng, et al. "Study of a harmonic drive with involute profile flexspline by two-dimensional finite element analysis." *Engineering Computations* (2017).
- [8]. Zhao, Jieliang, Shaoze Yan, and Jianing Wu. "Analysis of parameter sensitivity of space manipulator with harmonic drive based on the revised response surface method." *Acta Astronautica* 98 (2014): 86-96.
- [9]. Maiti, Rathindranath. "A novel harmonic drive with pure involute tooth gear pair." *J. Mech. Des.* 126.1 (2004): 178-182.
- [10]. Sahoo, Vineet, Bhabani Sankar Mahanto, and Rathindranath Maiti. "Stresses in flex gear of a novel harmonic drive with and without payload." *Australian Journal of Mechanical Engineering* 20.4 (2022): 1054-1068.

- [11]. Xu, Zhaoxiang, Yazhen Wang, and Haifeng Wang. "Calculation and Analysis of Deformation Characteristic and Energy Dissipation of Flexible Bearings in Harmonic Drive for Industrial Robots." *Journal of Physics: Conference Series*. Vol. 2365. No. 1. IOP Publishing, 2022.
- [12]. Huang, Jianzhong, et al. "Circumferential spatial tooth profile modification of flexspline for harmonic drive: A novel method and a case study." (2022).
- [13]. Kim, Beom-Seok, Seung-Tae Jeong, and Hyeong-Joon Ahn. "The Prediction of the Angular Transmission Error of a Harmonic Drive by Measuring Noncontact Tooth Profile and Considering Three-dimensional Tooth Engagement." *International Journal of Precision Engineering and Manufacturing* (2023): 1-8.
- [14]. Hrcek, Slavomir, et al. "Global sensitivity analysis of chosen harmonic drive parameters affecting its lost motion." *Materials* 14.17 (2021): 5057.
- [15]. Li, Yangfan, Gaoming Zhang, and Yingjie Zhang. "Thermal–mechanical coupling deformation difference analysis for the flexspline of a harmonic drive." *Reviews on Advanced Materials Science* 61.1 (2022): 698-710.
- [16]. Trang, ThanhTrung, et al. "A quick stress calculation method for flexspline in harmonic actuators based on the finite element method." *Cogent Engineering* 9.1 (2022): 2138123.
- [17]. Kim, Taesu, et al. "Development of Harmonic Drive Combining Four Arcs for Conventional Kinematic Application." *Machines* 10.11 (2022): 1058.
- [18]. Zhang, Yuxin, et al. "Calculating the Load Distribution and Contact Stress of the Disposable Harmonic Drive under Full Load." *Machines* 10.2 (2022): 96.
- [19]. Yang, Guo, et al. "Fault detection of harmonic drive using multiscale convolutional neural network." *IEEE Transactions on Instrumentation and Measurement* 70 (2020): 1-11.

- [20]. Ding, Muchuan. "Fast-slow Dynamical Analysis in Harmonic Gear Transmission System with Non-smooth Gear Clearance Condition." *Current Journal of Applied Science and Technology* 42.7 (2023): 66-75.
- [21]. Kuo, Jong-Yih, et al. "Constructing Condition Monitoring Model of Harmonic Drive." *Applied Sciences* 12.19 (2022): 9415.
- [22]. Tang, Ting, et al. "Modeling of transmission compliance and hysteresis considering degradation in a harmonic drive." *Applied Sciences* 11.2 (2021): 665.
- [23]. Hofmann, Douglas C., et al. "Castable bulk metallic glass strain wave gears: towards decreasing the cost of high-performance robotics." *Scientific reports* 6.1 (2016): 37773.
- [24]. Oh, Se Hoon, and Seung Hwan Chang. "Improvement of the dynamic properties of a steel-composite hybrid flexspline of a harmonic drive." *Composite Structures* 38.1-4 (1997): 251-260.
- [25]. Jeong, Kwang Seop, and Se Hoon Oh. "Development of the composite flexspline for a cycloid-type harmonic drive using net shape manufacturing method." *Composite Structures* 32.1-4 (1995): 557-565.
- [26]. Jeon, Han Su, and Se Hoon Oh. "A study on stress and vibration analysis of a steel and hybrid flexspline for harmonic drive." *Composite Structures* 47.1-4 (1999): 827-833.
- [27]. Fołęga, P., and G. Siwiec. "Numerical analysis of selected materials for flexsplines." *Archives of metallurgy and materials* 57 (2012): 185-191.
- [28]. Fołęga, Piotr. "Study of dynamic properties of composite and steel-composite flexsplines of harmonic drives." *Journal of Vibroengineering* 17.1 (2015): 155-163.
- [29]. Li, Y. B., et al. "Flow simulation of the effects of pressure angle to lobe pump rotor meshing characteristics." IOP Conference Series: Materials Science and Engineering. Vol. 52. No. 3. IOP Publishing, 2013.
- [30]. Kumar, Er. Amrit. "Steel: Properties, Different Types and Applications [Notes & PDF]." THEMECHANICALENGINEERING.COM, Jan. 2023, themechanicalengineering.com/steel-properties-different-types.

- [31]. Demir Çelik Mamülleri - Çelikler.
web.karabuk.edu.tr/myasar/demircelik/celikler
- [32]. Ibrahim, Auwal, et al. "Design of self-erecting tower for a wind turbine." *Int. J. Eng. Res. Technol* 6 (2020): 63-82.
- [33]. Vasiliev, Valery V., and Evgeny V. Morozov. *Mechanics and analysis of composite materials*. Elsevier, 2001.
- [34]. Rohatgi, Pradeep K. "Metal matrix composites." *Defence science journal* 43.4 (1993): 323.
- [35]. O'brien, R. L. 'Welding Handbook'. Welding Processes, vol. 2, American, 1991.
- [36]. Hu, Guyue, et al. "Influence of Materials on Dry Friction and Wear Performance of Harmonic Reducer Circular Spline." *Metals* 13.2 (2023): 378.
- [37]. Harmonic Drive® Strain Wave Gear - Zero Backlash | Harmonic Drive | Harmonic Drive. www.harmonicdrive.net/technology.
- [38]. Özel, T., Y. Karpat, and A. Srivastava. "Hard turning with variable micro-geometry PcBN tools." *CIRP annals* 57.1 (2008): 73-76.
- [39]. Sun, X. S., et al. "A multi-axial fatigue model for fiber-reinforced composite laminates based on Puck's criterion." *Journal of Composite Materials* 46.4 (2012): 449-469.
- [40]. Yahya, N. A., and Safa Hashim. "Stress analysis of steel/carbon composite double lap shear joints under tensile loading." *Proceedings of the Institution of Mechanical Engineers, Part L: Journal of Materials: Design and Applications* 230.1 (2016): 88-104.
- [41]. Kurowski, Paul M. *Finite element analysis for design engineers*. SAE International, 2022.
- [42]. HKS (2006). "ABAQUS Theory Manual."
- [43]. ABAQUS. "Abaqus user subroutines reference guide." *Abaqus Online Documentation* (2013).
- [44]. Abaqus, A. "ABAQUS online documentation." *Providence, RI, USA: Dassault Systemes Simulia Corporation* (2016).
- [45]. Campilho RDSG., Banea MD, Neto JABP, Da Silva LFM. Modelling adhesive joints with cohesive zone models: effect of the cohesive law shape of

- the adhesive layer. *International Journal of Adhesion and Adhesives* 2013; 44: 48-56.
- [46]. Saraç İ, Adin H, Temiz Ş. Investigation of the effect of use of nano-Al₂O₃, nano-TiO₂ and nanoSiO₂ powders on strength of single lap joints bonded with epoxy adhesive. *Compos Part B* 2019; 166: 472–482.
- [47]. Çitil Ş, Ayaz Y, Temiz Ş. Stress analysis of adhesively bonded double strap joints with or without intermediate part subjected to tensile loading. *J Adhes* 2017; 93(5):343–356.
- [48]. Barenblatt GI. The formation of equilibrium cracks during brittle fracture. General ideas and hypotheses. Axially-symmetric cracks. *Journal of Applied Mathematics and Mechanics* 1959; Vol. 23: 622-636.
- [49]. Dugdale DS. Yielding of steel sheets containing slits. *Journal of the Mechanics and Physics of Solids* 1960; 8: 100-104.
- [50]. Rice JR. A path independent integral and the approximate analysis of strain concentrations by notches and cracks. *Journal of Applied Mechanics* 1968; 35: 379-386.
- [51]. Çitil Ş. Investigation of curved and scarf lap joints subjected to tensile loads using the cohesive zone model. *Proceedings of the Institution of Mechanical Engineers, Part C: Journal of Mechanical Engineering Science* 2019; 233(17): 6149-6156.
- [52]. SARAÇ, İsmail. "YAPIŞTIRMA BAĞLANTILARINDA KOHEZİF BÖLGE MODELİ UYGULAYARAK VE UYGULAMADAN MODELLEME YAPILMASININ GERİLME DAĞILIMINA ETKİSİNİN ARAŞTIRILMASI." *Adıyaman Üniversitesi Mühendislik Bilimleri Dergisi* 8.15 (2021): 457-468.
- [53]. Salve, Ajinkya K., and Sudhindra N. Jalwadi. "Implementation of cohesive zone in ABAQUS to investigate fracture problems." *Proceedings of the National Conference for Engineering Postgraduates RIT, NConPG–15*. 2015.
- [54]. Gigerenzer, Gerd. "What are natural frequencies?" *Bmj* 343 (2011).

Ek A: Tez Fotokopisi İzin Formu

Anabilim Dalı:

YAZARIN

Soyadı :

Adı :

Bölümü :

TEZİN ADI (İngilizce) :

TEZİN TÜRÜ : Yüksek Lisans

Doktora

1. Tezimin tamamından kaynak gösterilmek şartıyla fotokopi alınabilir.
2. Tezimin içindekiler sayfası, özet, indeks sayfalarından ve/veya bir bölümünden kaynak gösterilmek şartıyla fotokopi alınabilir.
3. Tezimden bir bir (1) yıl süreyle fotokopi alınamaz.

TEZİN KÜTÜPHANEYE TESLİM TARİHİ:

